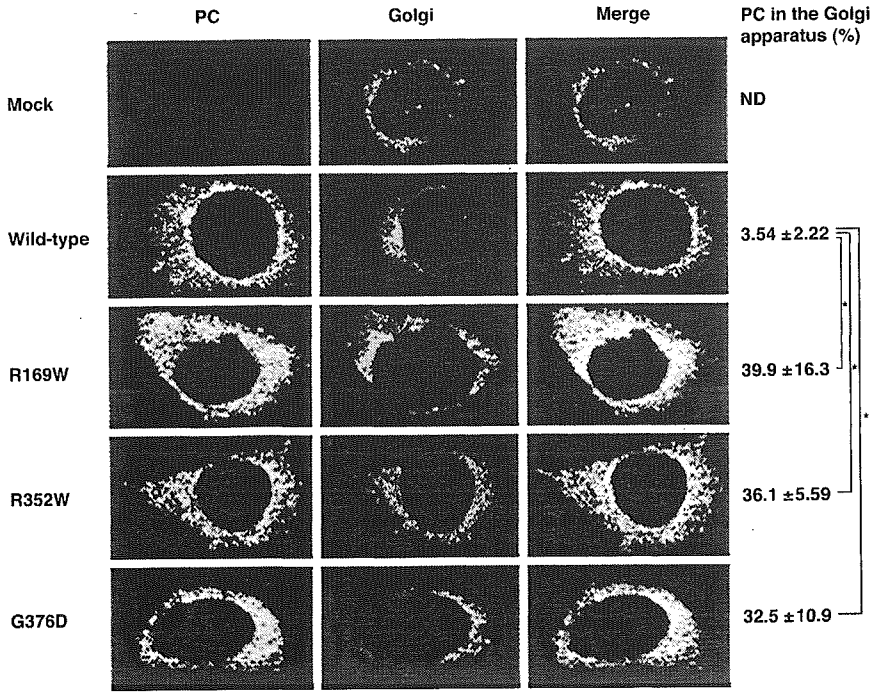

Figure 3. Cellular localization of wild-type PC and PC mutants. Cells expressing wild-type PC and mutant PC (R169W, R352W, or G376D) were incubated in the presence of fluorescently labeled sphingolipids (red), followed by immunofluorescence detection of PC antigen (green) using a confocal laser microscopy as described in Materials and Methods. Mock-transfected cells (Mock) were processed simultaneously as the control. The images were merged for evaluation of regions of colocalization (yellow). After quantitative analysis, the yellow area (PC colocalized with the Golgi apparatus) was expressed as the percentage of the green area (intracellular PC) and was shown in the right side of images (PC in the Golgi apparatus: mean±SD, n=4). *$P<0.01$ for differences between areas of colocalization. ND indicates not determined.

but the rate of decrease inside the cells was slightly slower in PC G376D than in PC R169W and PC R352W (Figure 2D). This may be explained by the observation that PC G376D was not secreted at all and suggests that the rates of degradation of these mutant molecules were similar. Collectively, the overall data demonstrate that wild-type PC is secreted from cells immediately after γ-carboxylation and modification at the Golgi apparatus without degradation, whereas secretion of PC R169W, PC R352W, and PC G376D is severely or completely impaired, and the molecules are degraded inside the cells.

Cellular Localization of Wild-Type PC and PC Mutants

To study the localization of wild-type PC and the mutant PC in the cells, immunofluorescence colocalization studies were performed using two-color confocal microscopy. The transfected cells were incubated with BODIPY-TR ceramide, a fluorescent sphingolipid that is incorporated into the Golgi apparatus. The cells were then processed for PC antigen using anti-PC polyclonal antibody and Alexa-488–labeled anti-goat IgG. As shown in Figure 3, the majority of wild-type PC did not colocalize with the fluorescent signal in the Golgi apparatus, suggesting that the transit time in the Golgi for wild-type PC is fairly short. PC R169W and PC R352W appear to colocalize with the Golgi more than does wild-type PC, suggesting that these mutant PC molecules might be retained in the Golgi apparatus. PC G376D was not secreted from the cells at all, but this abnormal molecule also colocalized with the Golgi, suggesting that a certain amount of PC G376D was transported to the Golgi.

Glycosylation of Wild-Type PC and PC Mutants

[^{35}S]Methionine-labeled wild-type and PC mutants in the conditioned medium and in the cell extracts synthesized in the presence or absence of vitamin K were isolated by immunoprecipitation and treated with Endo H. Endo H hydrolyzes Asn-linked oligosaccharides with a mannose core.[22,23] However, Endo H is unable to hydrolyze complex oligosaccharides of glycoproteins once a modification, such as addition of sialic acid, takes place in the trans face of the Golgi apparatus. Thus, the resistance of oligosaccharide side chains to Endo H is thought to be a marker of the posttranslational processing of the glycoprotein in the trans face of the Golgi.[22,23] As expected, oligosaccharides of wild-type and mutant PC in the conditioned medium were resistant to Endo H (Figure 4), suggesting that their carbohydrate side chains were complex oligosaccharides. In the presence of warfarin, less wild-type PC was secreted into the media, but their oligosaccharides were Endo H resistant, suggesting that γ-carboxylation was not mandatory for modification of oligosaccharides in the Golgi apparatus. PC R169W and PC R352W were partly secreted in the presence of vitamin K but were not secreted at all in the presence of warfarin. The majority of wild-type PC in the cell extracts was sensitive to Endo H and was converted to the deglycosylated form (indicated by an asterisk) by Endo H treatment. Thus, the majority of wild-type PC found in the cell extracts did not undergo modification of carbohydrate side chains at the trans face of the Golgi apparatus. The presence of vitamin K or warfarin did not affect the susceptibility of oligosaccharide side chains of wild-type PC in the cell extracts to Endo H. However, the amount of PC secreted into the conditioned medium in the presence of warfarin was less than that in the presence of vitamin K. When cells were cultured in the presence of vitamin K, PC R169W and PC R352W in the cell extracts were converted to the deglycosylated form by Endo H, and populations that migrated slower than the deglycosylated form of wild-type PC were observed (double asterisk), indicating that this population of PC R169W and PC R352W

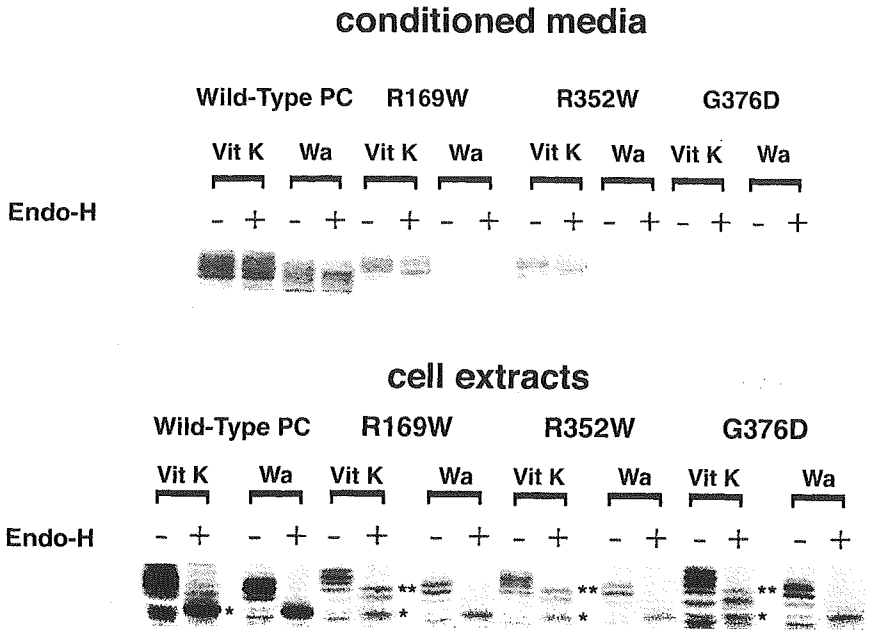

Figure 4. Analysis of carbohydrate side chains of wild-type PC and mutant PC. Stably transfected CHO-K1 cells expressing wild-type PC and PC mutants were incubated in medium containing [^{35}S]methionine for 1 hour, washed, and incubated in the standard medium in the presence of vitamin K (Vit K) or warfarin (Wa) as described in Materials and Methods. PC molecules in the cell extracts obtained after 1 hour of labeling and those in the conditioned medium, harvested after 8 hours of incubation, were isolated by immunoprecipitation. After dissociation of PC from Sepharose-CL4B by heating in the presence of SDS, samples were incubated in the presence or absence of 0.1 U/mL Endo H for 16 hours. These samples were analyzed by SDS-PAGE, followed by autoradiography. *Deglycosylated PC. **Endo H–resistant PC.

had undergone modification of oligosaccharide side chains in the trans face of the Golgi apparatus. In the presence of warfarin, PC R169W and PC R352W in the cell extracts were converted to the deglycosylated form and were not secreted into the conditioned medium. Similarly, PC G376D in the cell extracts had complex oligosaccharide side chains when cells were cultured in the presence of vitamin K. Taken together, these data support the notion that wild-type PC is secreted rapidly from cells on modification of the oligosaccharide side chain in the Golgi apparatus. In contrast, the PC mutants are retained inside the cells, even after modification of oligosaccharide side chains in the trans face of Golgi apparatus, and γ-carboxylation of the Gla domain of PC is necessary for efficient transport of PC from the endoplasmic reticulum (ER) to the Golgi apparatus.

Discussion

A variety of genetic abnormalities are responsible for PC deficiency (type I) and abnormalities (type II) associated with thrombotic episodes, and many reports have shown that even single amino acid substitutions can cause a type I PC deficiency.[11–15] On the basis of analyses of synthesis rates, posttranslational modifications, and secretion of wild-type PC and mutant PC with single amino acid substitution, we demonstrated that conformational defects resulted in the impaired sorting of abnormal molecules to secretory vesicles in the trans-Golgi network. This impairment may be at least partly responsible for PC deficiency caused by single amino acid substitution.

Because the majority of wild-type PC in the cell extracts did not bind to JTC3 monoclonal antibody and did not localize with the Golgi apparatus and because the oligosaccharides were sensitive to Endo H, wild-type PC appeared to reside mainly in the rough endoplasmic reticulum (RER) and was secreted quickly once it underwent modification at the Golgi, as reported previously.[24] According to the ELISA and pulse-chase data, secretion of the three PC mutants was impaired. Only small amounts of PC R169W and PC R352W were secreted, and PC G376D was not secreted at all from the cells. In contrast to wild-type PC, a portion of the PC mutants was retained inside the cells even after receiving oligosaccharide side chain modification at the Golgi apparatus. The observation that PC R169W and PC R352W colocalized with the Golgi to a greater extent than did wild-type PC also supports this notion. Data indicate that binding of PC G376D to JTC4 (epitope: catalytic domain) is decreased, whereas binding to JTC5 (epitope: activation peptide) is increased, supporting the notion that the conformation of the G376D mutant, in which secretion is completely abolished, is perturbed more severely than it is for the two other mutants. Taken together, these data indicate that an abnormal conformation induced in the catalytic domain of PC, together with an additional conformational change of the Gla domain, results in a secretion defect of mutant PC molecules to secretory vesicles in the trans-Golgi network.

Intracellular protein transport is a complex process coordinated by a variety of molecules. Compared with protein transport from RER to the Golgi apparatus by the ER quality control machinery, the regulatory mechanisms of protein transport from the Golgi apparatus to secretory vesicles and to cell surfaces are not well understood. Recently, the presence of sorting receptors and their important roles in protein transport from the Golgi have been proposed.[25,26] An association of secretory proteins with sorting receptors and/or trans-Golgi network membranes may be important in proteins for secretion.[27] Thus, a transport defect in abnormal molecules could reside in the trans-Golgi network. Impaired transport of an abnormal PC from the RER to the Golgi apparatus was proposed for the type I deficiency that is due to an abnormal PC molecule that has a substitution of the 39 carboxyl-terminal amino acids with 81 meaningless residues caused by a frame-shift mutation.[24] Although it was difficult to quantify PC molecules at each transport step in the present

study, decreased transport of PC R169W, PC R352W, and PC G376D mutants from the RER to the Golgi apparatus by the ER quality control mechanism might partly account for the impaired secretion of these molecules because these abnormal molecules appeared to have a conformational defect(s). The Endo H digestion study also clearly showed that Endo H–resistant abnormal molecules resided in the cell extracts, suggesting that retention of abnormal molecules in the Golgi apparatus did exist. In addition, data indicating that PC G376D, which was not secreted from the cells at all, was colocalized with the Golgi apparatus suggested that this abnormal molecule was transported from the RER to the Golgi and then retained. Thus, defective sorting to secretory vesicles in the trans-Golgi network would also be partly responsible for the patient with PC deficiency. To our knowledge, this is the first demonstration of a defect in the transport of a vitamin K–dependent protein from the Golgi apparatus to secretory vesicles.

In addition to binding to a sorting receptor for regulated secretory proteins, association of proteins to the membrane of the trans-Golgi network is thought to be necessary for the segregation of proteins to secretory vesicles.[27] In that context, the difference in reactivity to the JTC3 monoclonal antibody between the mutant PC molecules in the cell extracts and in the conditioned medium was interesting. PC R169W and PC R352W were not secreted well, but the majority of those PC molecules that were secreted were bound to JTC3. However, PC R169W and PC R352W in the cell extracts did not bind to JTC3 at all, even though certain amounts of these molecules were transported to the trans-Golgi apparatus.

Like other vitamin K–dependent coagulation factors, PC undergoes posttranslational processing.[9] As well as N-linked glycosylation, γ-carboxylation of vitamin K–dependent proteins is thought to take place before transport to the Golgi apparatus and possibly as a cotranslation event in the RER. Because the PC mutants in the present study have an amino acid substitution in the catalytic domain, cotranslational γ-carboxylation[8] of the Gla domain of these molecules is likely to be processed properly. Inasmuch as mutant PC in the cell extracts did not bind to JTC3 antibody, the amino acid substitutions in the catalytic domain may have affected the molecular chaperone–dependent appropriate folding of the Gla domain, which may contribute to the impaired secretion of these molecules.

When the cells were incubated in the presence of warfarin, the secretion of wild-type PC decreased, but the translation of wild-type PC was not decreased. The secreted noncarboxylated wild-type PC molecules were resistant to Endo H. Some of the mutant PC molecules in the cell extracts were retained even after oligosaccharide side chain modification at the Golgi apparatus because these were resistant to Endo H when the cells were cultured in the presence of vitamin K. However, these mutant molecules in the cell extracts were sensitive to Endo H, and no mutant PC molecules were present in the conditioned medium when the cells were cultured in the presence of warfarin. These data suggest that γ-carboxylation of PC is necessary for the efficient transport of PC from the ER to the Golgi apparatus but that it is not absolutely required for secretion from the cells. It is well known that vitamin K antagonist treatment causes not only secretion of dysfunctional vitamin K–dependent coagulation factors but also decreased plasma levels of these molecules, although the mechanism for the decreased plasma levels are not known. In accordance with previous studies,[28] data shown in the present study indicate that the primary cause of decreased secretion of vitamin K–dependent coagulation factors from the cells during vitamin K antagonist treatment is inefficient transport of these molecules from the RER to the Golgi apparatus.

In conclusion, an appropriate conformation of PC and other vitamin K–dependent factors is required for efficient transport from the RER to the Golgi apparatus and from the trans-Golgi apparatus to secretory vesicles. A conformational defect in the catalytic domain caused by single amino acid substitutions results in a type I deficiency, which is partly due to defective sorting of the abnormal molecules into secretory vesicles at the trans-Golgi network.

Acknowledgments

This study was supported by grants-in-aid from the Ministry of Education and Scientific Research to Drs Mimuro and Sakata.

References

1. Dahlbäck B. The protein C anticoagulant system: inherited defects as basis for venous thrombosis. *Thromb Res.* 1995;77:1–43.
2. Kisiel W. Human plasma protein C: isolation, characterization, and mechanism of activation by α-thrombin. *J Clin Invest.* 1979;64:761–769.
3. Stenflo J. A new vitamin K-dependent protein: purification from bovine plasma and preliminary characterization. *J Biol Chem.* 1976;251: 355–363.
4. Foster D, Davie EW. Characterization of a cDNA coding for human protein C. *Proc Natl Acad Sci U S A.* 1984;81:4766–4770.
5. Foster DC, Yoshitake S, Davie EW. The nucleotide sequence of the gene for human protein C. *Proc Natl Acad Sci U S A.* 1985;82:4673–4677.
6. Grinnell BW, Walls JD, Gerlitz B. Glycosylation of human protein C affects its secretion, processing, functional activities, and activation by thrombin. *J Biol Chem.* 1991;266:9778–9785.
7. Foster DC, Rudinski MS, Schach BG, Berkner KL, Kumar AA, Hagen FS, Sprecher CA, Insley MY, Davie EW. Propeptide of human protein C is necessary for γ-carboxylation. *Biochemistry.* 1987;26:7003–7011.
8. Furie B, Furie BC. Molecular basis of vitamin K-dependent γ-carboxylation. *Blood.* 1990;75:1753–1762.
9. McClure DB, Walls JD, Grinnell BW. Post-translational processing events in the secretion pathway of human protein C, a complex vitamin K-dependent antithrombotic factor. *J Biol Chem.* 1992;267: 19710–19717.
10. Ohlin AK, Landes G, Bourdon P, Oppenheimer C, Wydro R, Stenflo J. β-Hydroxyaspartic acid in the first epidermal growth factor-like domain of protein C: its role in Ca^{2+} binding and biological activity. *J Biol Chem.* 1988;263:19240–19248.
11. Reitsma PH, Poort SR, Allaart CF, Briet E, Bertina RM. The spectrum of genetic defects in a panel of 40 Dutch families with symptomatic protein C deficiency type I: heterogeneity and founder effects. *Blood.* 1991;78: 890–894.
12. Alhenc-Gelas M, Gandrille S, Aubry ML, Aiach M. Thirty-three novel mutations in the protein C gene: French INSERM network on molecular abnormalities responsible for protein C and protein S. *Thromb Haemost.* 2000;83:86–92.
13. Doig RG, Begley CG, McGrath KM. Hereditary protein C deficiency associated with mutations in exon IX of the protein C gene. *Thromb Haemost.* 1994;72:203–208.
14. Miyata T, Sakata T, Zheng YZ, Tsukamoto H, Umeyama H, Uchiyama S, Ikusaka M, Yoshioka A, Imanaka Y, Fujimura H, Kambayashi J, Kato H. Genetic characterization of protein C deficiency in Japanese subjects using a rapid and nonradioactive method for single-strand conformational polymorphism analysis and a model building. *Thromb Haemost.* 1996; 76:302–311.

15. Reitsma PH, Bernardi F, Doig RG, Gandrille S, Greengard JS, Ireland H, Krawczak M, Lind B, Long GL, Poort SR, Saito H, Sala N, Witt I, Cooper D, on behalf of the Subcommittee on Plasma Coagulation Inhibitors of the Scientific and Standardization Committee of the ISTH. Protein C deficiency: a database of mutations, 1995 update. *Thromb Haemost.* 1995; 73:876–889.
16. Mimuro J, Muramatsu S, Kaneko M, Yoshitake S, Iijima K, Nakamura K, Sakata Y, Matsuda M. An abnormal protein C (protein C Yonago) with an amino acid substitution of Gly for Arg-15 caused by a single base mutation of C to G in codon 57 (CGG to GGG). *Int J Hematol.* 1993; 57:9–14.
17. Sugahara Y, Miura O, Yuen P, Aoki N. Protein C deficiency Hong Kong 1 and 2: hereditary protein C deficiency caused by two mutant alleles, a 5-nucleotide deletion and a missense mutation. *Blood.* 1992;80:126–133.
18. Mimuro J, Sakata Y, Wakabayashi K, Matsuda M. Level of protein C determined by combined assays during disseminated intravascular coagulation and oral anticoagulation. *Blood.* 1987;69:1704–1711.
19. Wakabayashi K, Sakata Y, Aoki N. Conformation-specific monoclonal antibodies to the calcium-induced structure of protein C. *J Biol Chem.* 1986;261:11097–11105.
20. Nakamura S, Sakata Y. Immunoaffinity purification of protein C by using conformation-specific monoclonal antibodies to protein C-calcium ion complex. *Biochim Biophys Acta.* 1987;925:85–93.
21. Matsuda M, Sugo T, Sakata Y, Murayama H, Mimuro J, Tanabe S, Yoshitake S. A thrombotic state due to an abnormal protein C. *N Engl J Med.* 1988;319:1265–1268.
22. Kornfeld R, Kornfeld S. Assembly of asparagine-linked oligosaccharides. *Annu Rev Biochem.* 1985;54:631–664.
23. Maley F, Trimble RB, Tarentino AL, Plummer TH Jr. Characterization of glycoproteins and their associated oligosaccharides through the use of endoglycosidases. *Anal Biochem.* 1989;180:195–204.
24. Katsumi A, Senda T, Yamashita Y, Yamazaki T, Hamaguchi M, Kojima T, Kobayashi S, Saito H. Protein C Nagoya, an elongated mutant of protein C, is retained within the endoplasmic reticulum and is associated with GRP78 and GRP94. *Blood.* 1996;87:4164–4175.
25. Cool DR, Normant E, Shen F, Chen HC, Pannell L, Zhang Y, Loh YP. Carboxypeptidase E is a regulated secretory pathway sorting receptor: genetic obliteration leads to endocrine disorders in Cpe(fat) mice. *Cell.* 1997;88:73–83.
26. Baron CL, Malhotra V. Role of diacylglycerol in PKD recruitment to the TGN and protein transport to the plasma membrane. *Science.* 2002;295: 325–328.
27. Tooze SA, Martens GJ, Huttner WB. Secretory granule biogenesis: rafting to the SNARE. *Trends Cell Biol.* 2001;11:116–122.
28. Tokunaga F, Wakabayashi S, Koide T. Warfarin causes the degradation of protein C precursor in the endoplasmic reticulum. *Biochemistry.* 1995; 34:1163–1170.

[CANCER RESEARCH 63, 5091–5094, August 15, 2003]

Interleukin-10-mediated Inhibition of Angiogenesis and Tumor Growth in Mice Bearing VEGF-producing Ovarian Cancer[1]

Takahiro Kohno, Hiroaki Mizukami, Mitsuaki Suzuki, Yasushi Saga, Yuji Takei, Masahisa Shimpo, Takashi Matsushita, Takashi Okada, Yutaka Hanazono, Akihiro Kume, Ikuo Sato, and Keiya Ozawa[2]

Division of Genetic Therapeutics, Center for Molecular Medicine [T. K., H. M., Y. S., Y. T., M. S., T. M., T. O., Y. H., A. K., K. O.] and Department of Obstetrics and Gynecology [M. S., Y. S., Y. T., I. S.], Jichi Medical School, Tochigi, 329-0498 Japan

ABSTRACT

Interleukin-10 (IL-10) is an immunosuppressive cytokine produced by T lymphocytes and drawing attention as an inhibitor of tumor angiogenesis. In this study, we investigated antiangiogenic and tumor suppressive effects of IL-10 in ovarian cancer cells. mIL-10-expressing plasmid was transferred into two ovarian cancer cell lines, SHIN-3 [vascular endothelial growth factor (VEGF) producing] and KOC-2S (non-VEGF producing). After selection, mIL-10-expressing cells were obtained as SHIN-3/mIL-10 and KOC-2S/mIL-10. No significant differences were observed in *in vitro* growth properties between mIL-10-expressing cells and control (luciferase expressing) cells in either KOC-2S or SHIN-3. The angiogenic activities of mIL-10-expressing cells were measured by dorsal air sac assay, which detected the number of newly formed blood vessels within a chamber *in vivo*. In addition, tumor formation was evaluated by s.c. tumor transplantation, and survival was monitored after i.p. injection of ovarian cancer cells into BALB/c nude mice. Both *in vivo* angiogenic activity and tumor growth were significantly inhibited in SHIN-3/mIL-10 cells compared with the control. Moreover, peritoneal dissemination was inhibited, and the survival period was significantly prolonged (mean survival days > 90 *versus* 36). In contrast, in the case of KOC-2S cells, no significant differences were observed in any of the parameters tested. These results indicate that IL-10 has suppressive effects on angiogenesis, tumor growth, and peritoneal dissemination of VEGF-producing ovarian cancer cells. Although the mechanisms of the antiangiogenic effect of IL-10 are still unclear, the potential usefulness of IL-10-mediated gene therapy of ovarian cancer was suggested.

INTRODUCTION

Ovarian cancer has been on the increase in recent years and is currently a leading cause of death from gynecologic malignancy (1). Ovarian cancer is relatively asymptomatic and first detected as an advanced disease with ascites and peritoneal dissemination in more than half of patients (2). Although the progress of anticancer agents, such as platinum analogues and paclitaxel, has improved therapeutic response in advanced ovarian cancer, the long-term prognosis remains unsatisfactory (3). In the case of ovarian cancer, peritoneal dissemination is the most common form of progression and recurrence (2), and both the size of disseminated tumors and amount of ascitic fluid are known to correlate inversely with the prognosis (4). Therefore, the control of peritoneal dissemination is crucial to improve the prognosis.

The growth and spread of malignant neoplasms largely depend on angiogenesis (5, 6). Angiogenesis in ovarian cancer also plays a major role in the growth of disseminated tumors (7). Thus, inhibition of angiogenesis may not only suppress peritoneal dissemination and growth of the disseminated lesions but also improve the prognosis for advanced ovarian cancer.

In addition to being known as an immunosuppressive cytokine, IL-10[3] has recently been reported to have angiogenesis inhibitory activity (8, 9). We focused on this action of IL-10 and investigated the inhibition of peritoneal dissemination through angiogenesis inhibition by IL-10 both *in vitro* and *in vivo* using an IL-10-transduced human ovarian cancer cell line.

MATERIALS AND METHODS

Cell Lines and Plasmids. The human ovarian serous adenocarcinoma cell lines SHIN-3 (10) provided by Dr. Y. Kiyozuka (Hyogo College of Medicine, Japan), and KOC-2S (11) provided by Dr. A. Kataoka (Kurume University, School of Medicine, Japan) were maintained as reported. Cloned mIL-10 cDNA was inserted into the *Bam*HI site of the plasmid pCMV-IRES-bsr (12). Then either the plasmid pCMV-mIL-10-IRES-bsr or the control plasmid pCMV-LUC-IRES-bsr (12) encoding LUC were transferred into SHIN-3 and KOC-2S cells by the standard calcium phosphate precipitation method (13). The cells were selected in the presence of 10 μg/ml blasticidin S hydrochloride (Funakoshi, Tokyo, Japan). Resistant clones were obtained after 4 weeks and named as SHIN-3/mIL-10, SHIN-3/LUC, KOC-2S/mIL-10, and KOC-2S/LUC, respectively. The cells were subsequently maintained in the presence of 10 μg/ml blasticidin S hydrochloride.

Confirmation of mIL-10 Secretion and VEGF Quantitation. Conditioned media from 5×10^6 of cells in 10 ml of serum-free DMEM:F12 medium (Life Technologies, Inc., Grand Island, NY) in 10-cm dishes were collected at 24 h. Western blotting was performed under standard procedures (14) using anti-mIL10 monoclonal antibody (Genzyme, Cambridge, MA). VEGF concentrations of cultured supernatants were measured with a Quantikine Human VEGF ELISA kit (R&D Systems) according to the manufacturer's instructions.

***In Vitro* Cell Growth Kinetics and *in Vivo* Tumor Growth.** Both mIL-10-expressing and control cells were plated in 3-cm dishes at 5×10^4 cells/dish and cultured subsequently in 10% serum-supplemented DMEM/F12 medium. Every 24 h, one set of the cells was dislodged using 0.05% trypsin-EDTA and counted by hemocytometer. To investigate the effect of mIL-10 expression on tumor growth, 5×10^6 cells were s.c. transplanted on the back of the female BALB/c nude mice (Japan Clea Laboratories, Tokyo, Japan) at 4 weeks of age. Six days after transplantation, two dimensions of the tumors were measured using a caliper every 3 days. The tumor volume was estimated with the equation $[\text{width}]^2 \times [\text{length}] \times 1/2$. All of the animal experiments were performed under the guidelines of Jichi Medical School.

Dorsal Air Sac Assay. The angiogenic activities of mIL-10-expressing cells and control cells were measured by dorsal air sac assay as described previously (15). Briefly, diffusion chambers (Millipore Co., Bedford, MA) were filled with each of the suspension of cells (3×10^6) in 150 μl of PBS. The cell-containing chamber was implanted into the preformed s.c. air sac in the dorsum of an anesthetized female BALB/c nude mouse. On day 5, the implanted chambers were removed from treated mice. The angiogenic response was assessed by determining the number of newly formed vessels >3 mm in length within the area marked by a black ring. As described previously (15), the blood vessels formed by angiogenic factors released from tumor cells were morphologically distinct from the pre-existing background vessels.

Received 11/7/02; revised 4/14/03; accepted 6/5/03.

The costs of publication of this article were defrayed in part by the payment of page charges. This article must therefore be hereby marked *advertisement* in accordance with 18 U.S.C. Section 1734 solely to indicate this fact.

[1] Supported in part by grants from the Ministry of Health, Labor and Welfare of Japan; grants-in-aid for Scientific Research from the Ministry of Education, Culture, Sports, Science and Technology, Japan; and a grant-in-aid of the Japan Medical Association.

[2] To whom requests for reprints should be addressed, at Division of Genetic Therapeutics, Center for Molecular Medicine, Jichi Medical School, 3311-1 Yakushiji, Minamikawachi, Tochigi, 329-0498 Japan.

[3] The abbreviations used are: IL-10, interleukin-10; CMV, cytomegalovirus; IRES, internal ribosome entry site; VEGF, vascular endothelial growth factor; *bsr*, blasticidin S resistance gene; mIL-10, murine interleukin-10; LUC, luciferase.

***In Vivo* Ascites Accumulation, Peritoneal Dissemination, and Survival Rate.** BALB/c nude mice, maintained under a pathogen-free environment, were inoculated i.p. with either mIL-10-expressing cells or control cells at 5×10^6 cells/body. Two and 3 weeks after the i.p. injection, the mice were sacrificed; 1 ml of PBS was injected i.p., and the ascites fluid was recovered totally. Peritoneal dissemination was evaluated by counting the number of tumor nodes on the surface of the small intestine. Survival of the mice was monitored twice daily. The survival rate was calculated by the Kaplan-Meier method.

Statistical Analysis. All experiments were independently repeated twice or more. The significance of differences were analyzed by unpaired Student's *t* test. The survival rates were analyzed by the generalized Wilcoxon and Log-rank tests. A value of $P < 0.05$ was defined as statistically significant.

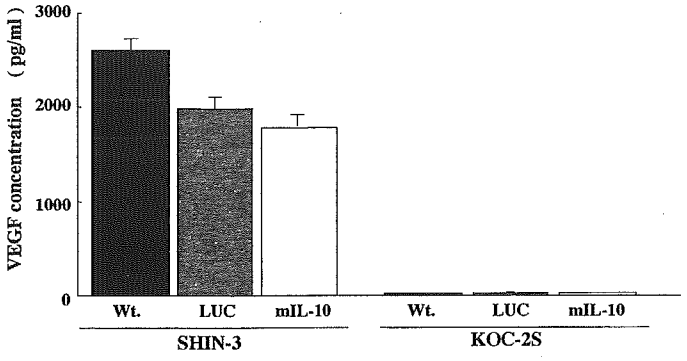

Fig. 1. Quantitation of VEGF in culture supernatant. mIL-10-expressing cells and control cells were plated in wells (5×10^6 cells/well) and cultured in serum-free medium for 24 h. SHIN-3 cells produced VEGF in contrast to KOC-2S cells. There were no significant differences between transduced and wild-type cells. The data represent the mean ± SD based on triplicate experiments.

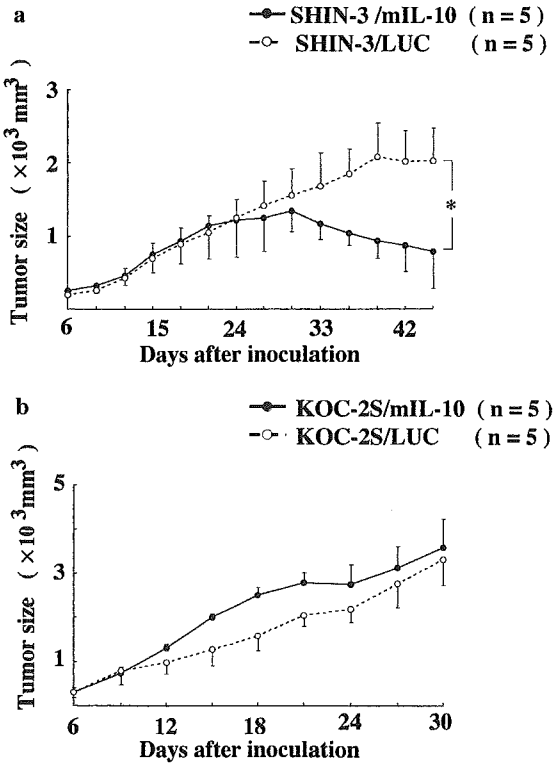

Fig. 2. *In vivo* tumor growth of mIL-10-expressing cells. Tumor cells were s.c. injected into the back of mice and measured every 3 days. In *a*, the tumor size of SHIN-3/mIL-10 (●) at 45 days after inoculation was $0.8 \pm 0.5 \times 10^3$ mm^3, which was significantly smaller than SHIN-3/LUC (○; $2 \pm 0.4 \times 10^3$ mm^3; *, $P < 0.05$). In *b*, the tumor growth curves of KOC-2S/mIL-10 (●) and KOC-2S/LUC (○) did not show significant differences. The tumor volumes were calculated based on the equation [width]^2 × [length] × 1/2 (mm^3). The data represent the mean ± SD.

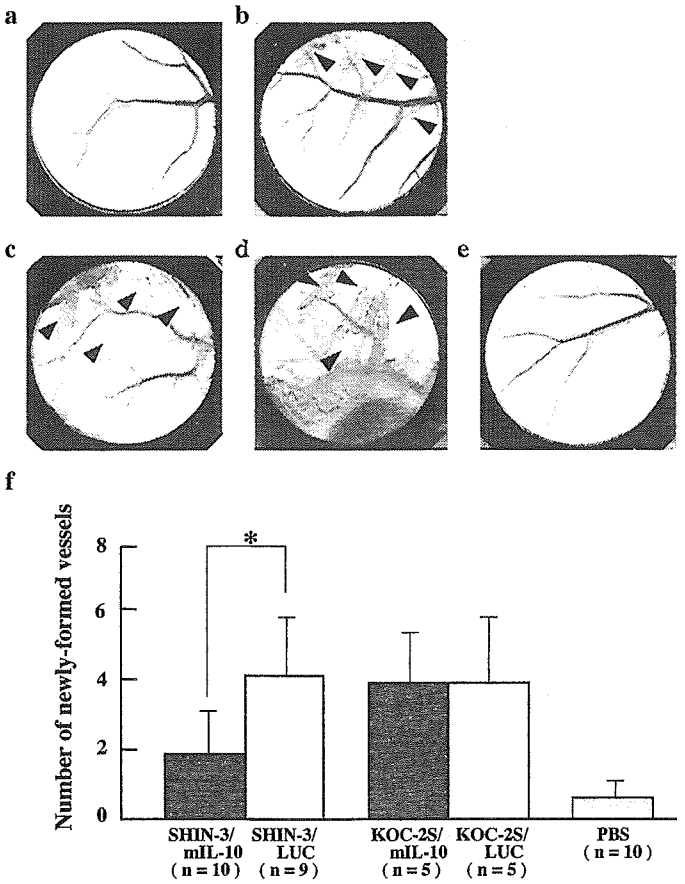

Fig. 3. Angiogenic response induced by tumor cells. Chambers containing SHIN-3/mIL-10 (*a*) and KOC-2S/mIL-10 (*c*) were implanted s.c. into mice. Chambers containing SHIN-3/LUC (*b*) and KOC-2S/LUC (*d*) were implanted as control group. Chambers containing only PBS (*e*) were implanted as vehicle-treated group. Newly formed vessels induced by SHIN-3 cells were mostly abolished by mIL-10 expression (*a*). *Arrowheads* point to newly formed vessels. Photographs were taken at day 5. The angiogenic response was assessed by counting the number of newly formed vessels longer than 3 mm(f). The numbers of newly formed vessels are significantly reduced in the case of SHIN-3/mIL-10 (1.9 ± 1.2) compared with the case of SHIN-3/LUC (4.22 ± 1.72). KOC-2/mIL-10 and KOC-2S/LUC did not show significant differences. Each bar represents the mean ± SD. *, $P < 0.05$.

RESULTS

Expression of mIL-10 and VEGF Concentration in Culture Supernatant. Either the mIL-10-expressing plasmid vector pCMV-mIL-10-IRES-bsr or the control vector (pCMV-LUC-IRES-bsr) was transferred into the SHIN-3 and KOC-2S cell lines, and the clones were developed. The presence of mIL-10 in the culture supernatant of mIL-10-transfected cells was confirmed by Western blotting. In contrast, no mIL-10 could be detected from culture supernatants of control cells (data not shown). Fig. 1 shows VEGF concentrations in culture supernatants from SHIN-3 and KOC-2S cells. The wild-type SHIN-3 cells were VEGF hypersecretory (2607 ± 124 pg/ml), whereas the wild-type KOC-2S cells were not (20 ± 4 pg/ml). There were no significant differences in the level of VEGF secretion between the mIL-10-transfected SHIN-3 or KOC-2S cell line and the corresponding control, showing that mIL-10 expression did not influence the VEGF secretion by tumor cells *in vitro*.

***In Vitro* Cell Growth Kinetics.** These mIL-10-transduced cells and the control cells were microscopically indistinguishable and had similar growth rates *in vitro*. No differences were noted in either the SHIN-3 or KOC-2S cell line. Therefore, the expression of the mIL-10 gene did not influence the tumor cell growth *in vitro* (data not shown).

***In Vivo* Tumor Growth.** On the basis of the results of *in vitro* experiments, we investigated the effect of mIL-10 expression on tumor growth *in vivo*. As shown in Fig. 2*a*, SHIN-3/mIL-10 tumors tend to shrink from day 30 after inoculation, significantly smaller than the control on day 45 [$(0.8 \pm 0.5) \times 10^3$ mm^3 *versus* $(2 \pm 0.4) \times 10^3$ mm^3, $P < 0.05$]. In contrast, KOC-2S/mIL-10 tumors did not show a difference from the control (Fig. 2*b*). These results indicate that mIL-10 expression suppressed SHIN-3 tumor growth.

Dorsal Air Sac Assay. We examined the effect of mIL-10 expression on angiogenesis by dorsal air sac assay. The number of newly formed vessels in chambers filled with PBS alone (negative control) was 0.6 ± 0.52, and little or no angiogenic response occurred after experimental manipulation or during the subsequent healing process (Fig. 3*e*). The number of newly formed vessels in SHIN-3/LUC tumors separated by a semipermeable filter (positive control) was 4.22 ± 1.72 (Fig. 3*b*). However, as shown in Figs. 3, *a* and *f*, the number of newly formed vessels in SHIN-3/mIL-10 tumors was significantly decreased (1.9 ± 1.2, $P < 0.05$) compared with that in SHIN-3/LUC tumors. These results indicate that, in SHIN-3 cells, mIL-10 expression suppresses the SHIN-3-induced angiogenesis. In contrast, mIL-10 expression did not significantly influence angiogenesis in KOC-2S cells *in vivo* (Figs. 3, *c*, *d*, and *f*).

***In Vivo* Ascites Accumulation, Peritoneal Dissemination, and Survival Kinetics.** To investigate the effect of persistent mIL-10 expression on peritoneal dissemination and ascites accumulation, we injected either mIL-10-transduced cells or control cells into nude mice i.p. The mean volume of ascitic fluid in the SHIN-3/mIL-10-injected group was significantly smaller than that in the control group (0.73 ± 0.15 ml *versus* 2.8 ± 0.4 ml, $P < 0.05$; Fig. 4*a*). As the peritoneal dissemination, gross tumor nodes on small intestines in the SHIN-3/mIL-10-injected group were significantly decreased (6.7 ± 2.5 *versus* 96 ± 14.5, $P < 0.05$; Fig. 4*b*). In contrast, there were no significant differences in the mean volume of ascitic fluid or number of peritoneal disseminations between the KOC-2S/mIL-10-injected group and positive control group (Fig. 4, *a* and *b*).

In the SHIN-3/LUC-injected group, marked ascites accumulation was observed around day 20 after i.p. injection, and all mice died within 48 days after injection. In contrast, in the SHIN-3/mIL-10-injected group, the ascites accumulation was suppressed, and a significantly longer survival was observed ($P < 0.05$; Fig. 4*c*). On the other hand, there were no significant differences in the survival duration between the KOC-2S/mIL-10-injected group and control group (Fig. 4*d*). These results indicate that, specifically in SHIN-3 cells, persistent mIL-10 expression suppresses ascites production and peritoneal dissemination and prolongs mouse survival.

DISCUSSION

In this study, mIL-10 expression in a VEGF-hypersecretory cell line resulted in suppression of *in vivo* tumor growth, peritoneal dissemination, ascites accumulation, and prolonged survival in a mouse model of peritoneal dissemination. Presumably, the mechanism of the difference with these results was related to the angiogenesis-inhibitory activity of IL-10, because angiogenic activity was significantly suppressed in mIL-10-overexpressing SHIN-3/mIL-10 cells. In addition, the finding that mIL-10 expression had little effect on the VEGF-hyposecretory cell line KOC-2S suggests that the angiogenesis inhibitory activity of mIL-10 is mediated by VEGF. Investigating the mechanism of the VEGF-mediated angiogenesis inhibitory activity of mIL-10 in an experiment with mIL-10 knockout mice, Silvestre *et al.* (8) reported that IL-10 inhibited angio-

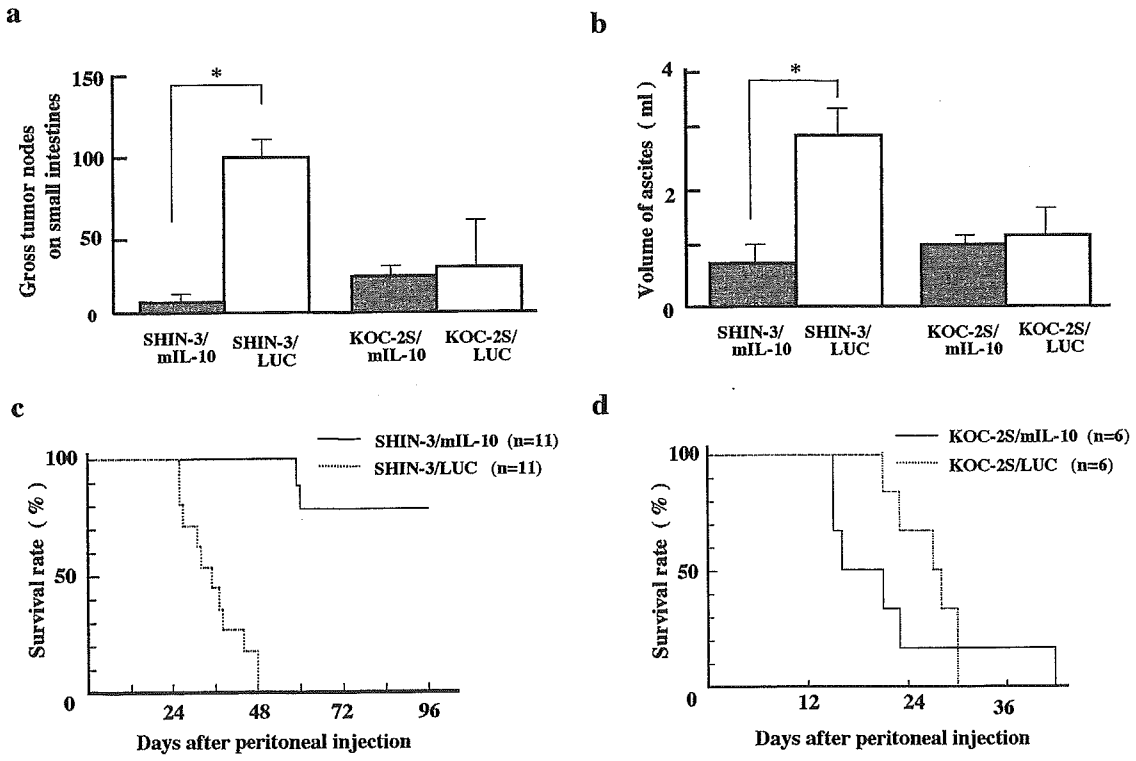

Fig. 4. Peritoneal dissemination, ascites accumulation, and survival kinetics of mIL-10-expressing cells. Tumor cells, 5×10^6 each, were i.p. injected into mice. In *a*, peritoneal dissemination at 3 weeks after injection was significantly less extensive in SHIN-3/mIL-10 (6.7 ± 2.5) than SHIN-3/LUC (96 ± 14.5). In *b*, ascites accumulation 3 weeks after injection was significantly reduced in SHIN-3/mIL-10 (0.73 ± 0.15 ml) compared with SHIN-3/LUC group (2.8 ± 0.4 ml). In *c*, the survival of mice injected with SHIN-3/mIL-10 was significantly longer than that of mice injected with SHIN-3/LUC ($P < 0.01$, by generalized Wilcoxon and Log-rank tests). No significant differences were observed in peritoneal dissemination, ascites accumulation, and survival kinetics between KOC-2S/mIL-10 and KOC-2S/LUC at 2 weeks after injection (*a*, *b*, and *d*). The data represent the mean $\pm$ SD based on triplicate experiments. *, $P < 0.05$.

genesis by down-regulating VEGF production. In an experiment with a human umbilical endothelial cell line, Cervenak *et al.* (9) found that IL-10 inhibits angiogenesis by competitively inhibiting VEGF. These observations, including our present study, suggest that mIL-10 inhibits angiogenesis through VEGF. However, the mechanism by which mIL-10 inhibits VEGF is yet to be elucidated and awaits further study.

Although this study found that IL-10 inhibited the growth and peritoneal dissemination of ovarian cancer, the application of IL-10 in clinical practice will require a prolonged, persistent expression. Therefore, it is desirable to transfer the IL-10 gene into a certain tissue and establish a gene therapy system. Because IL-10 is a secretory protein, it is not necessary to directly transfer the gene into cancer cells; transfer into cells such as skeletal muscle or peritoneal cells and its expression may turn the cells into "a factory" from which IL-10 is secreted into circulation to exert its effect. We consider that AAV vectors (9), which allow efficient gene transfer into a variety of cells, are suitable for implementing this strategy. We are in the process of testing its efficacy.

There may be further advantage in the use of IL-10 to treat cancer patients. In addition to angiogenesis inhibitory activity, IL-10 has been reported to have the effect of improving cancerous cachexia through suppression of the production of tumor necrosis factor-α and other cytokines (16, 17); therefore, IL-10 holds promise for improving the patient's QOL not only through its direct effect on tumors but also through the improvement of cancerous cachexia.

In summary, this study suggests that IL-10 inhibits the growth and peritoneal dissemination of ovarian cancer through the inhibition of angiogenesis, leading to improved survival. It also suggests the possibility of a novel gene therapy method using IL-10 and targeted at inhibition of peritoneal dissemination.

ACKNOWLEDGMENTS

We thank Avigen, Inc. (Alameda, CA) for the AAV vector production system.

REFERENCES

1. Landis, S. H., Murray, T., Bolden, S., and Wingo, P. A. Cancer statistics, 1999. CA Cancer J. Clin., *49:* 8–31, 1999.
2. Heintz, A. P. Surgery in advanced ovarian carcinoma: is there proof to show the benefit? Eur. J. Surg. Oncol., *14:* 91–99, 1988.
3. McGuire, W. P. *et al.* Cyclophosphamide and cisplatin compared with paclitaxel and cisplatin in patients with stage III and stage IV ovarian cancer. N. Engl. J. Med., *334:* 1–6, 1996.
4. Roszkowski, P., Wronkowski, Z., Szamborski, J., and Romejko, M. Evaluation of selected prognostic factors in ovarian cancer. Eur. J. Gynaecol. Oncol., *14:* 140–145, 1993.
5. Folkmann, J. Tumor angiogenesis. Adv. Cancer Res., *43:* 175–203, 1985.
6. Folkmann, J. Angiogenesis in cancer, vascular, rheumatoid, and other disease. Nat. Med., *1:* 27–31, 1995.
7. Abulafia, O., Triest, W. E., and Sherer, D. M. Angiogenesis in primary and metastatic epithelial ovarian carcinoma. Am. J. Obstet. Gynecol., *177:* 541–547, 1997.
8. Silvestre, J. S., Mallat, Z., Levy, B. I. *et al.* Antiangiogenic effect of interleukin-10 in ischemia-induced angiogenesis in mice hindlimb. Circ. Res., *87:* 448–452, 2000.
9. Cervenak, L., Morbidelli, L., Bejarano, M. T. *et al.* Abolished angiogenicity and tumorigenicity of Burkitt lymphoma by interleukin-10. Blood, *96:* 2568–2573, 2000.
10. Imai, S., Kiyozuka, Y., Maeda, H., Noda, T., and Hosick, H. L. Establishment and characterization of a human ovarian serous cystadenocarcinoma. Cell line that produces the tumor markers CA-125 and tissue polypeptide antigen. Oncology, *47:* 177–184, 1990.
11. Kataoka, A., Yokota, D., Yakushiji, M., and Kojiro, M. Establishment and characterization of ovarian serous adenocarcinoma cell line (KOC-2S). Hum. Cell, *1:* 337, 1988.
12. Urabe, M. *et al.* A novel dicistronic AAV vector using a short IRES segment derived from hepatitis C virus genome. Gene, *200:* 157–162, 1997.
13. Wigler, M., Pellicer, A., Silverstein, S., and Axle, R. Biochemical transfer of single-copy eucaryotic genes using total cellular DNA as donor. Cell, *14:* 725–731, 1978.
14. Laemmli, U. K. Cleavage of structural proteins during the assembly of the head of bacteriophage T4. Nature (Lond.), *227:* 680–685, 1970.
15. Yonekura, K., Basaki, Y., Yamada, Y. *et al.* UFT and its metabolites inhibit the angiogenesis induced by murine renal cell carcinoma, as determined by a dorsal air sac assay in mice. Clin. Cancer Res., *5:* 2185–2191, 1999.
16. Fujiki, F., Mukaida, N., Matsushima K. *et al.* Prevention of adenocarcinoma colon 26-induced cachexia by interleukin 10 gene transfer. Cancer Res., *57:* 94–99, 1997.
17. Fiorentino, D. F., Zlotnik, A., O'Garra, A., *et al.* IL-10 inhibits cytokine production by activated macrophages. J. Immunol., *147:* 3815–3822, 1991.

Journal of General Virology (2003), 84, 2127–2132 DOI 10.1099/vir.0.19193-0

Short Communication

Positive and negative effects of adeno-associated virus Rep on AAVS1-targeted integration

Masashi Urabe,[1,2,4] Katsuhiro Kogure,[1,2] Akihiro Kume,[1,2] Yuko Sato,[3] Kiyotake Tobita[4] and Keiya Ozawa[1,2]

Correspondence
Masashi Urabe (at Division of Genetic Therapeutics)
murabe@jichi.ac.jp

[1]Division of Genetic Therapeutics, Center for Molecular Medicine, Jichi Medical School, 3311-1 Yakushiji, Minami-Kawachi, Tochigi 329-0498, Japan

[2]CREST, Japan Science and Technology Corporation (JST), Tochigi 329-0498, Japan

[3]Department of Intractable Diseases, Research Institute, International Medical Center of Japan, Tokyo 162-8655, Japan

[4]Department of Virology, Jichi Medical School, Tochigi 329-0498, Japan

Adeno-associated virus type 2 integrates preferentially into the AAVS1 locus on chromosome 19 of the human genome. It was reported previously that transfection with two plasmids, one for Rep and the other carrying a transgene flanked by inverted terminal repeats (ITRs), enables preferential integration of the latter into AAVS1. Aiming at increasing the frequency of AAVS1-specific integration, the Rep- to transgene-plasmid ratio necessary to achieve a higher frequency of site-specific integration was examined. 293 cells were co-transfected with the Rep78 plasmid and an ITR-flanked Neo gene at different ratios. G418-resistant clones were selected randomly. Extensive Southern blot analysis showed an optimum range of Rep78 expression. In that range, approximately 20 % of clones harboured the Neo gene at AAVS1. Excess Rep expression, however, resulted in 'abortive' integration of the Neo gene, a rearrangement of AAVS1 without transgene integration. Rep78 appeared to cause abortive integration more extensively than Rep68. Deleterious effects of the Rep protein on the AAVS1 locus should be considered to develop an improved AAVS1-targeted system.

Received 3 March 2003
Accepted 1 April 2003

Retrovirus vectors are used widely for gene therapy applications. However, the random integration of retrovirus vector sequences may cause insertional mutagenesis, and the accidental activation of proto-oncogenes cannot be prevented. Adeno-associated virus type 2 (AAV) is a non-pathogenic parvovirus being considered as a gene transfer vehicle (Berns & Giraud, 1996; Kotin, 1994; Muzyczka, 1992). The AAV genome, a linear single-stranded DNA of 4·7 kb long, integrates preferentially into a defined locus in the human genome, AAVS1, on chromosome 19 (19q13·3-qter) (Kotin *et al.*, 1990, 1992; Samulski *et al.*, 1991). AAV can provide a potentially ideal gene delivery system for site-specific integration.

Each end of the AAV genome consists of inverted terminal repeats (ITRs), which are required in *cis* for AAVS1-specific integration. The AAV *rep* gene encodes four overlapping non-structural proteins, Rep78, Rep68, Rep52 and Rep40, while the *cap* gene encodes structural Cap proteins. The unspliced and spliced transcripts from the p5 promoter encode Rep78 and Rep68. Either Rep78 or Rep68 plays a key role in AAVS1-specific integration, binding ITRs (Im & Muzyczka, 1989) and AAVS1 (Weitzman *et al.*, 1994) via tandem repeats of the GAGC tetramer (McCarty *et al.*, 1994). The mechanism of AAVS1-specific integration of AAV has not been elucidated fully. However, a model whereby integration proceeds via a circular intermediate of the AAV genome by a deletion-substitution mechanism has been proposed (Dyall & Berns, 1998; Linden *et al.*, 1996).

A structural difference between Rep78 and Rep68 is that Rep78 possesses a zinc finger-like motif at its carboxyl terminus. Both Rep proteins share essentially the same functions: strand-specific DNA binding (Im & Muzyczka, 1989), site-specific nicking and ATP-dependent helicase activity (Im & Muzyczka, 1990). Either Rep protein alone is sufficient for replication of the AAV genome (Hölscher *et al.*, 1994) and for AAVS1-specific integration (Surosky *et al.*, 1997). The multifunctional Rep proteins inhibit cellular transformation by heterologous genes (Labow *et al.*, 1987; Yang *et al.*, 1992) and suppress heterologous promoters, including the c-*fos*, c-*myc*, H-*ras* and LTR of human immunodeficiency virus type 1 (HIV-1) (Hermonat, 1991, 1994; Oelze *et al.*, 1994). The Rep proteins also modulate cell cycle-regulating proteins (Hermanns *et al.*, 1997). These results indicate that overexpression of Rep proteins has negative effects on cells and is, on occasion, lethal to cells.

0001-9193 © 2003 SGM *Printed in Great Britain*

AAV vectors lacking the *rep* gene fail to integrate into AAVS1, showing apparent random integration into the host chromosomal DNA (Kearns *et al.*, 1996). A non-viral plasmid-based system capable of integrating a transgene specifically into AAVS1 has been described; this was achieved by transferring the transgene flanked by the ITRs with transient expression of Rep78 or Rep68 (Balagué *et al.*, 1997; Pieroni *et al.*, 1998; Shelling & Smith, 1994; Surosky *et al.*, 1997; Tsunoda *et al.*, 2000). Thus, this system is safer than integrating retrovirus and AAV vectors randomly. A strategy utilizing two plasmids, one harbouring the transgene cassette between the ITR sequences and the other for Rep expression, allows only the transgene plasmid to integrate into the AAVS1 locus (Surosky *et al.*, 1997). This method successfully introduced the transgene into AAVS1 in haematopoietic K562 cells (Kogure *et al.*, 2001).

The frequency of AAVS1-specific integration by the plasmid-based methods has differed among studies. Shelling & Smith (1994) reported that 9 of 12 cell clones (75 %) obtained by transfecting HeLa or 293 cells with an AAV vector plasmid on which the Neo gene was placed under the control of the p40 promoter, the original promoter for Cap proteins, had rearranged AAVS1 and mentioned that approximately 50 % of the rearranged bands also hybridized to an AAV probe. Another strategy using one plasmid on which both a Rep cassette and an ITR-flanked transgene cassette were placed has targeted the transgene to AAVS1 in 6 of 21 (29 %) 293 cell clones (Balagué *et al.*, 1997). Similar methods applied to other cell lines, HeLa and Huh-7 cells, have been able to insert the transgene to AAVS1 in up to 20 % of clones (Lamartina *et al.*, 1998; Pieroni *et al.*, 1998). All the studies mentioned here used a one plasmid system and the p5 promoter for Rep expression.

Aiming at increasing the frequency of AAVS1-directed integration, we first examined whether AAVS1-specific integration depended on the levels of Rep protein expressed in cells. To control the expression of the cytotoxic Rep proteins, we chose to vary the amount of Rep plasmid DNA. 293 cells were transfected using the calcium phosphate precipitation method with 2, 0·4, 0·2, 0·04, 0·02 or 0 μg pCMVR78, which expresses Rep78 under the control of the CMV promoter (Surosky *et al.*, 1997), and 2 μg pWNeo (Rep : Neo ratio of 1, 0·2, 0·1, 0·02, 0·01 or 0). pWNeo bears a Neo gene under the control of the CMV promoter between the ITRs. To monitor the amount of plasmid DNA incorporated, extrachromosomal DNA was analysed by Southern blot with a plasmid backbone probe (Fig. 1a). As the amount of Rep plasmid decreased, signal intensities corresponding to pCMVR78 decreased gradually, whereas those corresponding to pWNeo changed little, indicating that the amount of plasmid DNA incorporated into the cells correlated with that used for transfection. Western analysis of the transfected 293 cells confirmed that the expression level of the Rep protein was a function of the amount of pCMVR78 (Fig. 1b).

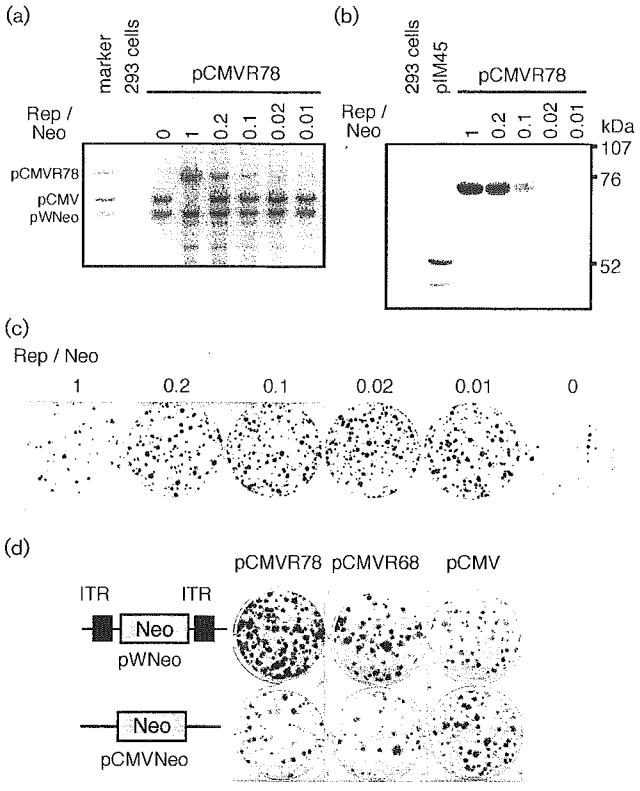

Fig. 1. (a) Quantification of plasmid DNAs incorporated into 293 cells. 293 cells (2×10^5 cells per well) in 6-well plates were transfected with 2 μg pWNeo and various amounts of pCMVR78 (0, 2, 0·4, 0·2, 0·04 or 0·02 μg) at a Rep to Neo plasmid ratio of 0, 1, 0·2, 0·1, 0·02 or 0·01 by the calcium phosphate precipitation method. The amount of plasmid DNA transfected per well was made up to a total of 4 μg with a plasmid devoid of a Rep cassette (pCMV). Following transfection, extrachromosomal DNA was isolated and treated with *Bam*HI. *Bam*HI digestion generates a 5·9, 3·4 or 4·0 kb band, derived from pCMVR78, pWNeo or pCMV, respectively, that hybridizes to a plasmid backbone probe. (b) Expression of Rep78 in 293 cells transfected with various amounts of pCMVR78. The Rep to Neo ratio is indicated above each lane. pIM45 harbours the AAV *rep* and *cap* genes (McCarty *et al.*, 1991). Anti-Rep antibody 294.4 (a gift from J. Kleinschmidt) was used. (c) Comparison of the number of G418-resistant colonies obtained using various amounts of pCMVR78. Following transfection with pCMVR78 and pWNeo at different Rep to Neo ratios (1, 0·2, 0·1, 0·02, 0·01 or 0 μg), a 1/500 fraction of transfected cells was replated onto a 10 cm dish in triplicate and cultured for 10 days in the presence of G418. (d) Representative comparison of the number of G418-resistant colonies generated using pCMVR78 or pCMVR68. After transfection with 0·8 μg pCMVR78, pCMVR68 or pCMV and 3·2 μg pWNeo or pCMVNeo, a 1/500 fraction of transfected cells was replated onto 6-well plates in triplicate and cultured for 10 days in the presence of G418. When either Rep plasmid was co-transfected with pWNeo, a larger number of colonies was formed.

Fig. 1(c) compares G418-resistant colonies grown after transfection with pCMVR78. The number of colonies increased significantly when pCMVR78 was added to the transfection solution. The number of colonies observed did not differ significantly at the Rep to Neo ratios of 0·2–0·01. On transfection at the Rep to Neo ratio of 1, however, the number of colonies decreased, probably due to the strong cytotoxicity of Rep78. To estimate the frequency of integration of the Neo gene to AAVS1, we extensively analysed clones by Southern blot. From each group, 14–20 clones were expanded and their genomic DNA was digested with *Hin*dIII or *Eco*RV, enzymes that do not cleave plasmid pWNeo or the proximal portion of AAVS1 where integration of the AAV genome occurs predominantly (Giraud *et al.*, 1994; Kotin *et al.*, 1992). The presence of co-migrating bands that hybridized to both AAVS1 and Neo probes on both *Hin*dIII- and *Eco*RV-blots was a criterion to conclude that the Neo gene was integrated into AAVS1. Table 1 summarizes the result of Southern blot analysis of the 293 cell clones. When the pCMVR78 to pWNeo ratio was 1 or 0·2, approximately 95 % of clones showed rearrangement of AAVS1. The frequency of rearrangement of AAVS1 decreased gradually as the amount of pCMVR78 was reduced. Unexpectedly, integration of the Neo gene into AAVS1 was observed only in 1 of 16 clones (6 %) at the Rep to Neo ratio of 1. In contrast, transfection at the Rep to Neo ratio of 0·2–0·02 produced approximately 20 % of clones that delivered the Neo gene to AAVS1. These results indicated that a high-level expression of the Rep proteins increased the frequency of AAVS1 rearrangement and rather decreased the frequency of AAVS1-specific integration of the transgene.

In the second experiment, we compared Rep78 with Rep68 by transfecting 0·8 μg pCMVR78, pCMVR68 or pCMV along with 3·2 μg pWNeo or pCMVNeo (Rep to Neo ratio of 0·25). pCMVR68 expresses Rep68 alone (Surosky *et al.*, 1997) and pCMVNeo is the same as pWNeo except for the absence of ITRs. Fig. 1(d) is a representative comparison of G418-resistant colony formation. The results of the Southern blot analysis of clones selected randomly are summarized in Table 1. Rep78 generated rearrangement of AAVS1 in approximately 90 % of clones and 24 % of clones had the Neo gene at AAVS1. The frequency of rearrangement of AAVS1 is 65 % with the use of pCMVR68 and 40 % of clones integrated the Neo gene to AAVS1. This result suggested that Rep78 appeared to cause more 'abortive' integration of the Neo gene, rearrangement of AAVS1 without integration of transgene, although the difference between Rep78 and Rep68 was not statistically significant.

Fig. 2 shows Southern blot analysis of representative clones with the Neo gene at AAVS1. Fig. 2(a, b) is the *Hin*dIII- or *Eco*RV-digest probed with an AAVS1-specific probe (upper panel) or a Neo probe (lower panel). Each clone presented here has an upshifted band(s) other than a basal band (arrow). Common bands that hybridized to both AAVS1 and Neo probes are indicated by arrowheads. Fluorescent *in situ* hybridization (FISH) analysis confirmed the integration of the Neo gene into chromosome 19 in 11 of 12 clones. A representative chromosomal analysis is shown in Fig. 2(c). The 293 cells used in the present study have four copies of chromosome 19 labelled with Cy-3-conjugated chromosome 19-specific probe (arrowheads). The left panel shows a metaphase spread of clone C6/6. Fluorescein Neo signals are localized to chromosome 19 and another unidentified site (arrows). In the right panel showing analysis of clone C6/18, one chromosome 19 harbours the Neo signals at its terminal portion.

'Abortive' integration into AAVS1, rearrangement of AAVS1 without foreign gene insertion, has been described in 293 or HeLa cells (Balagué *et al.*, 1997; Shelling & Smith,

Table 1. Summary of Southern blot analysis

	Experiment 1									Experiment 2			
Rep plasmid	**pCMVR78**									**pCMVR78**		**pCMVR68**	
Rep to Neo ratio	1		0·2		0·1		0·02		0·01	0·25		0·25	
No. of clones analysed	16		20		19		14		14	17		20	
Enzyme used	*Hin*dIII	*Eco*RV	*Hin*dIII	*Eco*RV	*Hin*dIII	*Eco*RV	*Hin*dIII	*Eco*RV	*Hin*dIII	*Hin*dIII	*Eco*RV	*Hin*dIII	*Eco*RV
Rearranged AAVS1 band*	14	14	19	18	14	8	9	7	6	13	15	12	13
Common band†	4	6	7	4	8	5	4	4	0	9	4	8	8
AAVS1 rearrangement (%)‡	15 (94)		19 (95)		14 (74)		9 (64)		6 (43)	15 (88)		13 (65)	
Neo at AAVS1(%)§	1 (6)		4 (20)		4 (21)		3 (21)		0 (0)	4 (24)		8 (40)	
Neo signal on chromosome 19‖										3		8	

*Number of clones with rearrangement of AAVS1.

†Number of clones with common bands hybridizing to both AAVS1 and Neo probes.

‡Number of clones with rearrangement of AAVS1 on either the *Hin*dIII or the *Eco*RV blot.

§Number of clones with common bands on both *Hin*dIII and *Eco*RV blots.

‖Number of clones with the Neo signal on chromosome 19.

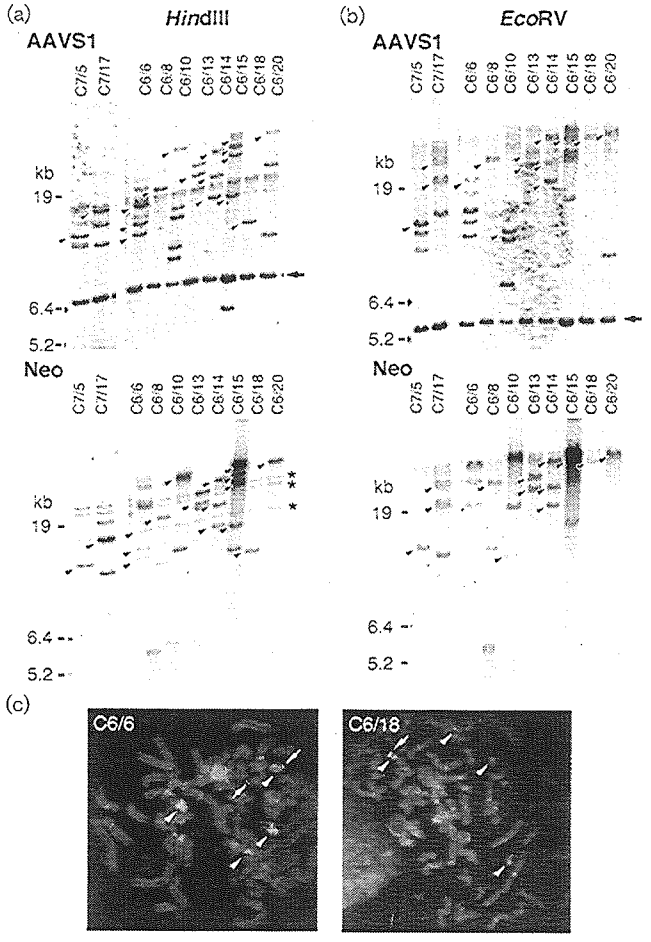

Fig. 2. Southern blot analysis of clones with the Neo gene at AAVS1. *Hin*dIII- or *Eco*RV-digested genomic DNA was hybridized initially with a ^{32}P-labelled AAVS1-specific probe [the 3·0 kb *Acc*I fragment from pRVK (a gift from K.I. Berns)]. After stripping the probe, membranes were rehybridized with a Neo-specific probe (the 2·0 kb *Not*I fragment derived from pWNeo). The presence of co-migrating bands that hybridized to both AAVS1 and Neo probes on both *Hin*dIII and *Eco*RV blots was a criterion to conclude that the Neo gene was integrated into AAVS1. (a) *Hin*dIII-digest probed with an AAVS1-specific probe (upper panel) or with a Neo probe (lower panel). (b) Blot of genomic DNA digested with *Eco*RV isolated from the same clones. Each clone presented here has an upshifted band(s) other than a basal 6·5 kb band (arrow). Common bands that hybridized to both AAVS1 and Neo probes are indicated by arrowheads. Asterisks indicate non-specific bands that cross-hybridized to the Neo probe used. Clones C7/5 and C/17 were derived from transfection with pCMVR78. Clones C6/6 to C6/20 were obtained using pCMVR68. (c) Representative FISH of clones shown to harbour the Neo gene at AAVS1 by Southern blot analysis. Note that the 293 cells used in the present study have four copies of chromosome 19 (arrowheads). Signals detected by a Neo probe (arrows) are indicated.

1994; Surosky *et al.*, 1997). A similar disruption of AAVS1 has been detected in cell lines latently infected with wild-type AAV (Kotin *et al.*, 1990). This phenomenon may be explained in three ways. First, the integrated transgene or AAV genome is disrupted during or after an integration event such that Southern blot analysis cannot detect it. The instability of the integrated AAV genome over passages in a latently infected cell line was described (Cheung *et al.*, 1980). An additional rearrangement can occur in the rearranged AAVS1 region (Shelling & Smith, 1994). Second, recombination between the AAVS1 region and other sites may cause rearrangement of AAVS1 without integration of the transgene at AAVS1. Third, the Rep protein may excise the integrated plasmid DNA or AAV genome, resulting in the loss of the preintegrated sequences.

The 293 cells used in the present study have four copies of chromosome 19. Southern blot analysis showed that some clones had more than three upshifted bands besides a basal band. We used a relatively large probe (3·0 kb) for detecting AAVS1 bands. It is possible that Rep-mediated disruption of the AAVS1 region can produce the multiple bands hybridizing to the AAVS1 probe. Another explanation is as follows: at 24 h post-transfection, we replated transfected cells to isolate clones derived from single cells. At this time-point, the Rep protein was still being expressed in cells and an additional integration event might occur in some cells after cell division.

Lamartina *et al.* (1998) reported no apparent difference between Rep78 and Rep68 in the ability to deliver foreign DNA to AAVS1 in HeLa cells. Several studies have reported the functional differences between Rep78 and Rep68. Rep68 is more efficient in processing dimers to monomer duplex DNA and possesses a stronger nicking activity (Ni *et al.*, 1994, 1998), while the helicase activity of Rep78 is stronger (Wollscheid *et al.*, 1997). The differential effects of Rep78 and Rep68 on the p5, p19 and p40 promoters were described (Weger *et al.*, 1997). In addition, Rep78 inhibits CREB-dependent transcription by interacting with protein kinase (Chiorini *et al.*, 1998; Di Pasquale & Stacey, 1998). None of these findings explains why Rep78 appears to cause more abortive integration. Rep68 may be more suitable for the AAVS1-targeted integration system. To confirm the usefulness of Rep68 in the AAVS1-targeted integration system, further analysis of a larger population of cell clones would be required. Also, the exact functions of the Rep protein in AAVS1-specific integration should be elucidated.

The results presented here have important implications for developing an AAVS1-directed integration system as well as for understanding the mechanism of AAVS1-specific integration by the Rep proteins.

ACKNOWLEDGEMENTS

We thank K. I. Berns for pRVK and J. A. Kleinschmidt for the anti-Rep antibody 294.4. This work was supported in part by grants from the Ministry of Health and Welfare of Japan, Grants-in-Aid for

Scientific Research from the Ministry of Education, Science, Sports and Culture of Japan, and Special Coordination Funds for Promoting Science and Technology of the Science and Technology Agency of the Japanese Government.

REFERENCES

Balagué, C., Kalla, M. & Zhang, W. W. (1997). Adeno-associated virus Rep78 protein and terminal repeats enhance integration of DNA sequences into the cellular genome. *J Virol* **71**, 3299–3306.

Berns, K. I. & Giraud, C. (1996). Biology of adeno-associated virus. *Curr Top Microbiol Immunol* **218**, 1–23.

Cheung, A. K., Hoggan, M. D., Hauswirth, W. W. & Berns, K. I. (1980). Integration of the adeno-associated virus genome into cellular DNA in latently infected human Detroit 6 cells. *J Virol* **33**, 739–748.

Chiorini, J. A., Zimmermann, B., Yang, L., Smith, R. H., Ahearn, A., Herberg, F. & Kotin, R. M. (1998). Inhibition of PrKX, a novel protein kinase, and the cyclic AMP-dependent protein kinase PKA by the regulatory proteins of adeno-associated virus type 2. *Mol Cell Biol* **18**, 5921–5929.

Di Pasquale, G. & Stacey, S. N. (1998). Adeno-associated virus Rep78 protein interacts with protein kinase A and its homolog PRKX and inhibits CREB-dependent transcriptional activation. *J Virol* **72**, 7916–7925.

Dyall, J. & Berns, K. I. (1998). Site-specific integration of adeno-associated virus into an episome with the target locus via a deletion-substitution mechanism. *J Virol* **72**, 6195–6198.

Giraud, C., Winocour, E. & Berns, K. I. (1994). Site-specific integration by adeno-associated virus is directed by a cellular DNA sequence. *Proc Natl Acad Sci U S A* **91**, 10039–10043.

Hermanns, J., Schulze, A., Jansen-Dürr, P., Kleinschmidt, J. A., Schmidt, R. & zur Hausen, H. (1997). Infection of primary cells by adeno-associated virus type 2 results in a modulation of cell cycle-regulating proteins. *J Virol* **71**, 6020–6027.

Hermonat, P. L. (1991). Inhibition of H-ras expression by the adeno-associated virus Rep78 transformation suppressor gene product. *Cancer Res* **51**, 3373–3377.

Hermonat, P. L. (1994). Down-regulation of the human c-*fos* and c-*myc* proto-oncogene promoters by adeno-associated virus Rep78. *Cancer Lett* **81**, 129–136.

Hölscher, C., Hörer, M., Kleinschmidt, J. A., Zentgraf, H., Bürkle, A. & Heilbronn, R. (1994). Cell lines inducibly expressing the adeno-associated virus (AAV) *rep* gene: requirements for productive replication of *rep*-negative AAV mutants. *J Virol* **68**, 7169–7177.

Im, D.-S. & Muzyczka, N. (1989). Factors that bind to adeno-associated virus terminal repeats. *J Virol* **63**, 3095–3104.

Im, D.-S. & Muzyczka, N. (1990). The AAV origin binding protein Rep68 is an ATP-dependent site-specific endonuclease with DNA helicase activity. *Cell* **61**, 447–457.

Kearns, W. G., Afione, S. A., Fulmer, S. B., Pang, M. C., Erikson, D., Egan, M., Landrum, M. J., Flotte, T. R. & Cutting, G. R. (1996). Recombinant adeno-associated virus (AAV-CFTR) vectors do not integrate in a site-specific fashion in an immortalized epithelial cell line. *Gene Ther* **3**, 748–755.

Kogure, K., Urabe, M., Mizukami, H., Kume, A., Sato, Y., Monahan, J. & Ozawa, K. (2001). Targeted integration of foreign DNA into a defined locus on chromosome 19 in K562 cells using AAV-derived components. *Int J Hematol* **73**, 469–475.

Kotin, R. M. (1994). Prospects for the use of adeno-associated virus as a vector for human gene therapy. *Hum Gene Ther* **5**, 793–801.

Kotin, R. M., Siniscalco, M., Samulski, R. J. & 7 other authors (1990). Site-specific integration by adeno-associated virus. *Proc Natl Acad Sci U S A* **87**, 2211–2215.

Kotin, R. M., Linden, R. M. & Berns, K. I. (1992). Characterization of a preferred site on human chromosome 19q for integration of adeno-associated virus DNA by non-homologous recombination. *EMBO J* **11**, 5071–5078.

Labow, M. A., Graf, L. H., Jr & Berns, K. I. (1987). Adeno-associated virus gene expression inhibits cellular transformation by heterologous genes. *Mol Cell Biol* **7**, 1320–1325.

Lamartina, S., Roscilli, G., Rinaudo, D., Delmastro, P. & Toniatti, C. (1998). Lipofection of purified adeno-associated virus Rep68 protein: toward a chromosome-targeting nonviral particle. *J Virol* **72**, 7653–7658.

Linden, R. M., Ward, P., Giraud, C., Winocour, E. & Berns, K. I. (1996). Site-specific integration by adeno-associated virus. *Proc Natl Acad Sci U S A* **93**, 11288–11294.

McCarty, D. M., Christensen, M. & Muzyczka, N. (1991). Sequences required for coordinate induction of adeno-associated virus p19 and p40 promoters by Rep protein. *J Virol* **65**, 2936–2945.

McCarty, D. M., Pereira, D. J., Zolotukhin, I., Zhou, X., Ryan, J. H. & Muzyczka, N. (1994). Identification of linear DNA sequences that specifically bind the adeno-associated virus Rep protein. *J Virol* **68**, 4988–4997.

Muzyczka, N. (1992). Use of adeno-associated virus as a general transduction vector for mammalian cells. *Curr Top Microbiol Immunol* **158**, 97–129.

Ni, T. H., Zhou, X., McCarty, D. M., Zolotukhin, I. & Muzyczka, N. (1994). *In vitro* replication of adeno-associated virus DNA. *J Virol* **68**, 1128–1138.

Ni, T. H., McDonald, W. F., Zolotukhin, I., Melendy, T., Waga, S., Stillman, B. & Muzyczka, N. (1998). Cellular proteins required for adeno-associated virus DNA replication in the absence of adenovirus coinfection. *J Virol* **72**, 2777–2787.

Oelze, I., Rittner, K. & Sczakiel, G. (1994). Adeno-associated virus type 2 *rep* gene-mediated inhibition of basal gene expression of human immunodeficiency virus type 1 involves its negative regulatory functions. *J Virol* **68**, 1229–1233.

Pieroni, L., Fipaldini, C., Monciotti, A. & 7 other authors (1998). Targeted integration of adeno-associated virus-derived plasmids in transfected human cells. *Virology* **249**, 249–259.

Samulski, R. J., Zhu, X., Xiao, X., Brook, J. D., Housman, D. E., Epstein, N. & Hunter, L. A. (1991). Targeted integration of adeno-associated virus (AAV) into human chromosome 19. *EMBO J* **10**, 3941–3950.

Shelling, A. N. & Smith, M. G. (1994). Targeted integration of transfected and infected adeno-associated virus vectors containing the neomycin resistance gene. *Gene Ther* **1**, 165–169.

Surosky, R. T., Urabe, M., Godwin, S. G., McQuiston, S. A., Kurtzman, G. J., Ozawa, K. & Natsoulis, G. (1997). Adeno-associated virus Rep proteins target DNA sequences to a unique locus in the human genome. *J Virol* **71**, 7951–7959.

Tsunoda, H., Hayakawa, T., Sakuragawa, N. & Koyama, H. (2000). Site-specific integration of adeno-associated virus-based plasmid vectors in lipofected HeLa cells. *Virology* **268**, 391–401.

Weger, S., Wistuba, A., Grimm, D. & Kleinschmidt, J. A. (1997). Control of adeno-associated virus type 2 cap gene expression: relative influence of helper virus, terminal repeats, and Rep proteins. *J Virol* **71**, 8437–8447.

Weitzman, M. D., Kyöstio, S. R., Kotin, R. M. & Owens, R. A. (1994). Adeno-associated virus (AAV) Rep proteins mediate complex

formation between AAV DNA and its integration site in human DNA. *Proc Natl Acad Sci U S A* **91**, 5808–5812.

Wollscheid, V., Frey, M., Zentgraf, H. & Sczakiel, G. (1997). Purification and characterization of an active form of the p78Rep protein of adeno-associated virus type 2 expressed in *Escherichia coli*. *Protein Expr Purif* **11**, 241–249.

Yang, Q., Kadam, A. & Trempe, J. P. (1992). Mutational analysis of the adeno-associated virus *rep* gene. *J Virol* **66**, 6058–6069.

THE JOURNAL OF GENE MEDICINE
J Gene Med 2003; 5: 438–445.
Published online 23 December 2002 in Wiley InterScience (www.interscience.wiley.com). **DOI:** 10.1002/jgm.356

RESEARCH ARTICLE

A DNA vaccine containing inverted terminal repeats from adeno-associated virus increases immunity to HIV

Ke-Qin Xin[1]
Takaaki Ooki[1]
Nao Jounai[1]
Hiroaki Mizukami[2]
Kenji Hamajima[1]
Yoshitsugu Kojima[1]
Kenji Ohba[1]
Yoshihiko Toda[1]
Syu-Ichi Hirai[3]
Dennis M. Klinman[4]
Keiya Ozawa[2]
Kenji Okuda[1]*

[1]*Department of Bacteriology, Yokohama City University School of Medicine, Yokohama 236-0004, Japan*

[2]*Division of Genetic Therapeutics, Center for Molecular Medicine, Jichi Medical School, Tochigi-ken 3290498, Japan*

[3]*Department of Biochemistry, Yokohama City University School of Medicine, Yokohama 236-0004, Japan*

[4]*Center for Biologics Evaluation and Research, US Food and Drug Administration, Bethesda, MD 20892, USA*

*Correspondence to:
Dr Kenji Okuda, Department of Bacteriology, Yokohama City University School of Medicine, 3–9 Fukuura, Kanazawa-ku, Yokohama 236-004 Japan. E-mail: kokuda@med.yokohama-cu.ac.jp

Received: 22 August 2002
Revised: 15 October 2002
Accepted: 24 October 2002

Abstract

Background DNA vaccines have been used to induce both humoral and cellular immune responses against infectious microorganisms. This study explores whether DNA vaccine immunogenicity can be improved by introducing inverted terminal repeats (ITRs) from adeno-associated virus (AAV) into the regulatory region of the DNA plasmid.

Methods CMV promoter-driven HIV Env expressing plasmid (pCMV-HIV) and the pCMV-HIV plasmid introduced ITRs (pITR/CMV-HIV) were transfected in HEK293 cells with LipofectAmine. The HIV Env expression was quantified with Western blot. Fifty μg of pCMV-HIV or pITR/CMV-HIV plasmid with RIBI adjuvant were immunized to BALB/c mice on days 0, 14 and 28 by intramuscular route, and HIV-specific serum IgG titer was detected 2, 6, 10, 14 and 18 weeks after the first immunization. HIV-specific tetramer assay and HIV-specific IFN-γ ELIspot assay were performed 1 week after the last immunization. The immune mice were intravenously challenged with a vaccinia virus expressing the HIV *env* gene 1 week after the last immunization.

Results Significantly higher level of HIV Env expression was achieved by pITR/CMV-HIV plasmid. BALB/c mice immunized with pITR/CMV-HIV plasmid generated significantly higher HIV-specific antibody, higher cellular immune responses and lower viral loading than animals immunized with pCMV-HIV plasmid.

Conclusions AAV ITRs enhance CMV-dependent up-regulation of transgene expression and immunogenicity of DNA vaccine. Copyright © 2002 John Wiley & Sons, Ltd.

Keywords AAV-ITR; DNA vaccine; immune response

Introduction

There is considerable interest in developing plasmid DNA vaccines to prevent or treat infectious diseases, including AIDS. However, results from clinical trials suggest that the immunogenicity of these vaccines in humans may be limited. To date, DNA vaccines alone have failed to prevent the replication of highly virulent HIV strains in non-human primates.

To increase the activity of this class of vaccine, we and others have been exploring the benefit of co-immunizing with various types of vaccine adjuvant [1–4]. Ongoing efforts to increase the immunogenicity of DNA

Copyright © 2002 John Wiley & Sons, Ltd.

vaccines include the co-delivery of vectors encoding immunomodulatory cytokines [1,5,6], chemokines [7], co-stimulatory molecules [8], CpG motif [4], chemical agents [2,9], and administering the DNA vaccine in lipid vesicles [10].

Can stronger DNA vaccines be constructed? This study investigates whether introducing inverted terminal repeats (ITRs) from adeno-associated virus (AAV) can improve the immunogenicity of DNA vaccines in a mouse model. AAV is a small, single-stranded DNA virus lacking an envelope. The 4.7-kb genome of AAV contains two 145-bp ITRs. Infected cells convert the single-stranded AAV DNA into a double-stranded transcriptional template which can then integrate into the genome of mammalian cells [11,12]. The AAV ITRs are *cis*-acting elements that promote AAV replication, integration, and excision, but which also enhance the activity of the AAV promoter [13].

To explore whether these ITRs can improve the function of the CMV promoter used to drive expression of the gene(s) encoded by DNA vaccines, plasmids were constructed that expressed either the HIV *env* or *lacZ* gene under the control of the CMV promoter with or without AAV ITRs. Results indicate that both *in vitro* and *in vivo*, addition of the ITRs enhances gene expression and the magnitude of the resultant immune responses.

Materials and methods

Plasmid DNA

The DNA plasmids used in this study are shown in Figure 1. The pCMV-LacZ plasmid was constructed as follows. A 2.7-kb *Kas* I-*Ear* I fragment from pUC19 was blunted and ligated to a multiple cloning sequence containing the restriction enzyme sites 5′-*Not* I-*Mlu* I-*Sna*B I-*Age* I-*Bst*B I-*Bss*H II-*Nco* I-*Hpa* I-*Bsp*E I-*Pml* I-*Rsr* II-*Not* I-3′. The following fragments were successively cloned into the following sites: a *Spe* I-*Sac* II fragment containing the cytomegalovirus (CMV) immediate-early promoter was cloned into the *Sna*B I site, a *Bst*B I-*Bst*B I fragment from the first intron of the human growth hormone was inserted into the *Bst*B I site, multi-cloning fragment (*Cla* I-*Eco*R I-*Sma* I-*Bam*H I-*Xba* I-*Acc* I-*Sal* I-*Bsp*M I-*Pst* I-*Eco*R V-*Xho* I-*Hind* III) was ligated into the *Bss*H II site, and the *Hpa* I-*Bam*H I fragment of the simian virus 40 (SV40) polyadenylation signal sequence was cloned into the *Hpa* I site (pCMV plasmid). The lacZ reporter gene was ligated into the *Eco*R I site of pCMV plasmid to generate pCMV-LacZ plasmid. The pITR/CMV-LacZ plasmid was constructed by inserting the *Not* I-*Not* I expression cassette from pCMV-LacZ plasmid between the AAV 145-bp ITRs of a pUC-based plasmid. The pITR-LacZ plasmid was constructed from a *Spe* I-*Cla* I fragment-deleted pITR/CMV-LacZ plasmid. To construct pCMV-HIV plasmid which expresses both HIV *env* and HIV *rev* genes, an internal ribosome entry site (IRES) fragment was ligated into the *Acc* I-*Bsp*M I site of the pCMV plasmid. Then a 2.5k bp full length HIV *env* gene and a 351 bp full length HIV *rev* gene amplified from pcREV were ligated into the *Eco*R I and *Pst* I-*Xho* I sites of the plasmid to generate the pCMV-HIV plasmid, respectively. The pITR/CMV-HIV plasmid was constructed by inserting the *Not* I-*Not* I expression cassette from the pCMV-HIV plasmid between the AAV 145-bp ITRs. The pITR-HIV plasmid was constructed from a *Spe* I-*Cla* I fragment-deleted pITR/CMV-HIV plasmid.

In vitro expression of the β-galactosidase and HIV *env* genes

Hela, Cos I and/or HEK 293 cells were transfected with 0.5, 2 or 5 μg of plasmid DNA (pCMV-LacZ, pITR/CMV-LacZ or pITR-LacZ) plus LipofectAmine Plus (Invitrogen) according to the manufacturer's instructions. Two days after transfection, gene expression was monitored in triplicate for each sample using a β-gal assay kit

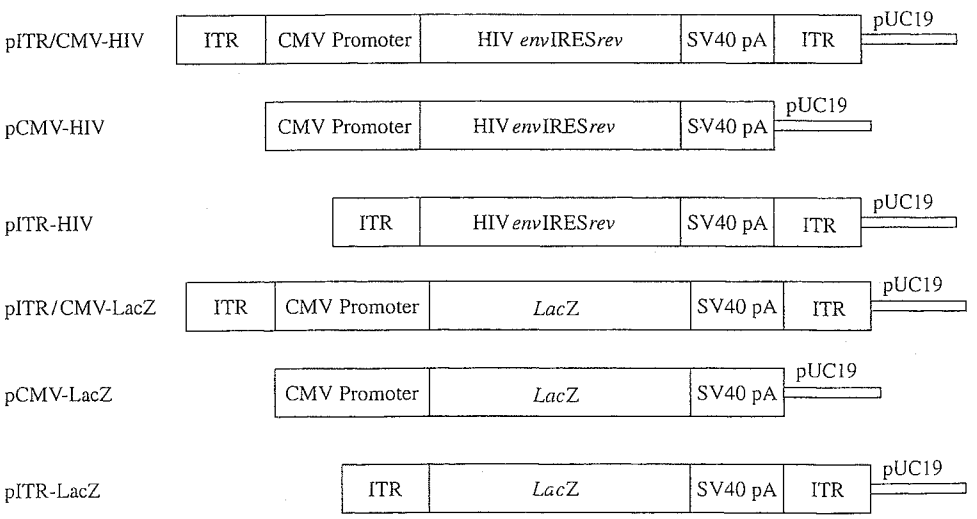

Figure 1. Organization of plasmids used in this study. ITR: inverted terminal repeat; CMV promoter: enhancer and CMV promoter; HIV *env*IRES*rev*: HIV *env*-IRES-HIV*rev*; SV40 pA: SV 40 polyadenylation signal sequence

Copyright © 2002 John Wiley & Sons, Ltd.

(Invitrogen) as recommended by the manufacturer. The β-galactosidase activity of cell lysates was calculated using a standard curve generated from a commercial enzyme preparation (*E. coli* β-galactosidase, Sigma).

To explore the transfection efficiency and integration or episomal persistence of ITR-introducing plasmid, at indicated time points post-transfection, part of the transfected cells was used for passage and remaining cells were used for detection of β-galactosidase activity and stained with X-gal. The β-galactosidase activity of cell lysates was calculated from the standard curve derived from the commercial enzyme preparation as above.

To quantify the expression of HIV Env protein, HEK 293 cells were transfected as described above with 0.5, 2 or 5 μg of plasmid (pCMV-HIV, pITR/CMV-HIV, pITR-HIV or pCMV-empty). Two days after transfection, the cells were washed in phosphate-buffered saline (PBS) and lysed in 50 mM Tris-HCl (pH 7.8) with 1% Nonidet P-40. The protein concentration of lysates was measured with a Bio-Rad protein assay kit. Cell lysates (10 μg) were loaded onto a 4–12% gradient polyacrylamide gel followed by transfer to Hybond ECL nitrocellulose membrane (Amersham Pharmacia Biotech, Bucks, UK). The protein was detected using the HIV-1 IIIB gp120 specific mouse hybridoma 902 (AIDS Research and Reference Reagent Program, MD, USA). An anti-β-actin mAb was used as an internal control antibody (AC-15; Sigma). An affinity-purified horseradish peroxidase (HRP)-labeled anti-mouse Ig Ab was used as the secondary Ab. The density of the protein bands was quantified using Image Gange software (version 3.0; Fujifilm, Tokyo, Japan). The ratio of HIV Env protein was calculated as (β-actin density of pITR/CMV-HIV × HIV Env density of pCMV-HIV)/β-actin density of pCMV-HIV). The HIV Env density included both density of gp120 and gp160.

Animals and animal immunization

Eight-week-old BALB/c female mice were purchased from Japan SLC. Inc. (Shizuoka, Japan). The mice were housed in the Animal Center of Yokohama City University where they were kept on a 12-h day/night cycle. Mice were intramuscularly immunized with 50 μg of plasmid plus 5 μl RIBI adjuvant in PBS on days 0, 14 and 28.

Sample collection and ELISA

Serum Abs were detected by ELISA, as previously described [14]. Briefly, 96-well microtiter plates were coated with 10 μg/ml of HIV V3 region peptide (NNTRKRIQRGPGRAFVTIGKIGN-multi-antigen peptide, HIV V3-MAP peptide) at 4 °C overnight. The wells were blocked with PBS containing 1% bovine serum albumin (BSA) and incubated for 2 h at room temperature. Serial two-fold dilutions of antisera were added for an additional hour at 37 °C. The bound Ab was detected using HRP-labeled anti-mouse IgG antibody (Sigma). The mean antibody titer was expressed as the reciprocal of the serial serum dilution that reached the cut-off value plus 2 SD.

IFN-γ ELIspot assay and computer-assisted video image analysis (CVIA)

IFN-γ ELIspot assays were performed 1 week after the final immunization, as previously described [15]. Briefly, MultiScreen-IP plates (Millipore, Bedford, MA, USA) were coated with 50 μl of 10 μg/ml of rat anti-mouse IFN-γ antibody in PBS (XMG1.2; Pharmingen, CA, USA) overnight at 4 °C. The plate was then blocked with RPMI1640 medium with 10% FCS for 2 h at room temperature. Lymphocytes ($1-10 \times 10^5$) from the spleen were added to each well, in triplicate. To monitor HIV-specific IFN-γ production, spleen cells were stimulated with 10 μg/ml of HIV V3 peptide (NNTRKRIQRGPGRAFVTIGKIGN) for 20 h at 37 °C. Control wells contained non-stimulated cells. After incubation, cells were removed and the wells incubated with 0.5 μg/ml of biotinylated anti-mouse IFN-γ antibody (Pharmingen) for 2 h at 37 °C, followed by adding 100 μl/well of 0.2% alkaline phosphatase streptavidin (Vector, CA, USA) in PBS containing 0.05% Tween-20 and 0.5% BSA for 1.5 h. Finally, the plate was treated with 50 μl/well of BCIP/NBT membrane phosphatase (Kirkegaare and Perry Laboratories, MD, USA) at room temperature for 20 min and the reaction was stopped under running distilled water. The numbers of spots were automatically determined by CVIA [16].

Tetramer assay

The tetramer assay was performed 1 week after the final boost. The H-2D/p18 tetramer (RGPGRAFVTI) labeled with PE was provided by the NIH AIDS Research and Reference Reagent Program. The H-2k(d)/NP tetramer (TYQRTRALV, influenza NP gene, PR8 strain) was used as a negative control tetramer reagent. The tetramer assay was performed as previously described [17]. Briefly, mouse splenocytes were incubated for 30 min at 4 °C with 4% normal mouse serum in PBS. Cells were stained with fluorescein isothiocyanate (FITC)-labeled anti-mouse CD8a antibody (Ly-2, Pharmingen) at 0.5 μg/10^6 cells for 30 min at 4 °C. After being washed twice with staining buffer (3% FCS, 0.1% NaN_3 in PBS), the cells were incubated with the tetramer reagent for 15 min at 37 °C followed by flow cytometric analysis.

Recombinant vaccinia virus used for challenge studies

The virus challenge experiment was performed 1 week after the last immunization as described previously [18]. Recombinant vaccinia virus vPE16 expressing the HIV-1 *env* gene (Cat. No. 362; NIH AIDS Reagent Program

Copyright © 2002 John Wiley & Sons, Ltd.

and Reference Reagent Program) was used for the study. Briefly, 1 week after immunization, mice were challenged intravenously with 5×10^7 plaque-forming units (pfu) of vPE16 vaccinia virus. Six days after the challenge with the recombinant vaccinia virus, the mice were sacrificed, and ovaries were removed, sonicated, and assayed for vPE16 titer by plating serial 10-fold dilution on a plate of CV1 cells, staining with crystal violet and counting plaques at each dilution.

Data analysis

All values are expressed as means ± standard error (S.E.). Statistical analysis of the experimental data and controls was conducted with one-way factorial analysis of variance. Significance was defined at $p < 0.05$ in statistical analyses.

Results

Addition of ITRs improves gene expression by DNA plasmids

To examine the effect of AAV ITRs on transgene expression, we prepared several constructs. As shown in Figure 1, the pITR/CMV-HIV and pCMV-HIV express full length of the HIV *env* and *rev* genes, which was controlled by CMV promoter with or without ITRs; the pITR-HIV contains AAV ITRs but lacks the CMV promoter. The HIV gene was replaced with a reporter gene, *lac*Z, to generate pITR/CMV-LacZ, pCMV-LacZ and pITR-LacZ for qualifying the protein expression. Hela, Cos I and HEK 293 cells were transfected with 2 μg each of pITR/CMV-LacZ, pCMV-LacZ or pITR-LacZ plasmid using LipofectAmine. Two days later, β-galactidase protein levels were measured. As seen in Figure 2, β-galactosidase activity was greatest in all three kinds of cell types transfected with pITR/CMV-LacZ, suggesting that the addition of the ITR to the pCMV-LacZ construct enhanced gene expression. Cells transfected with pITR-LacZ expressed no detectable enzyme activity. To explore whether the β-galactosidase activity was dependent on DNA plasmid dose, we transfected with 0.5 or 5 μg each of *lac*Z-containing DNA plasmid. A similar pattern of β-galactosidase activity was observed as with the one transfected with 2 μg of DNA plasmid (data not shown). This set of observations suggests that the ITR acts to enhance CMV promoter function, which is independent of the transfected DNA plasmid dose.

The HIV Env protein expression of plasmids was also quantified by Western blot. HEK 293 cells were transfected with 2 μg each of pITR/CMV-HIV, pCMV-HIV, pITR-HIV or mock pCMV plasmid. Results indicate that pITR/CMV-HIV-tranfected cells produced 1.8-fold more Env than pCMV-HIV-transfected cells (Figure 3). No HIV Env protein was detected in cells transfected with the

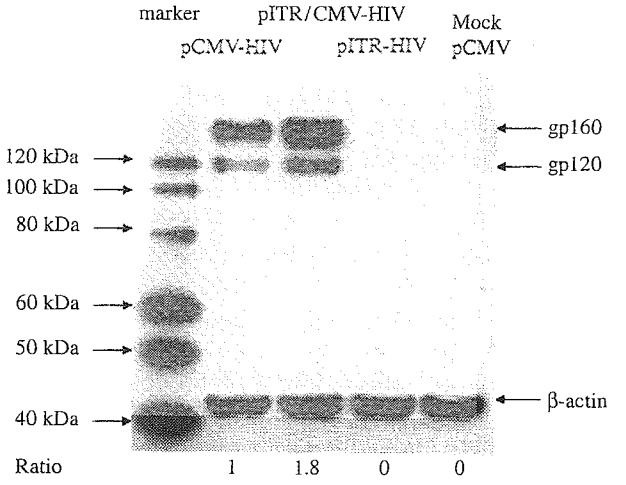

Figure 3. Quantification of HIV Env protein by Western blot. DNA plasmid (2 μg each) was transfected into HEK 293 cells. The amount of HIV Env protein in the lysates of HEK 293 cells transfected 2 days earlier was analyzed by Western blot. When 0.5 or 5 μg of DNA plasmid was used, HIV Env expression ratio of pITR/CMV-HIV to pCMV-HIV was similar to using 2 μg of DNA plasmid. Another two separate experiments showed similar results

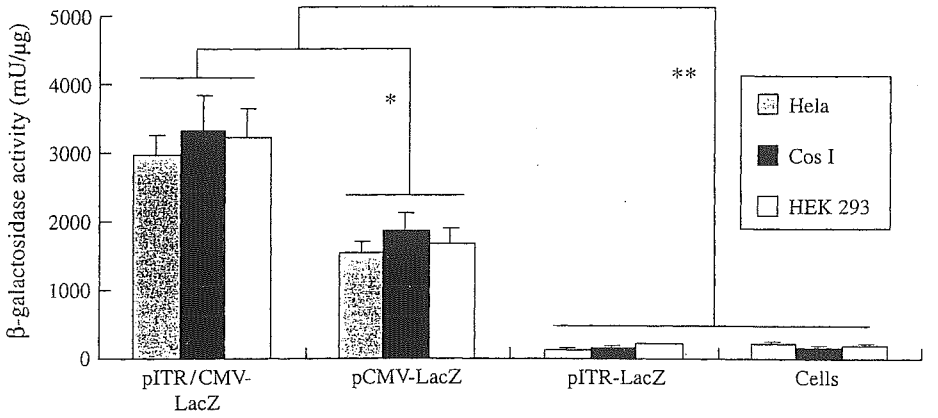

Figure 2. β-Galactosidase activity in transfected cell lines. The β-galactosidase activity was measured 2 days after LipofectAmine-mediated transfection of DNA plasmid, in triplicate for each sample. Data represent the average of 2–3 separate experiments. *, **Mean values significantly different from the two groups

Copyright © 2002 John Wiley & Sons, Ltd.

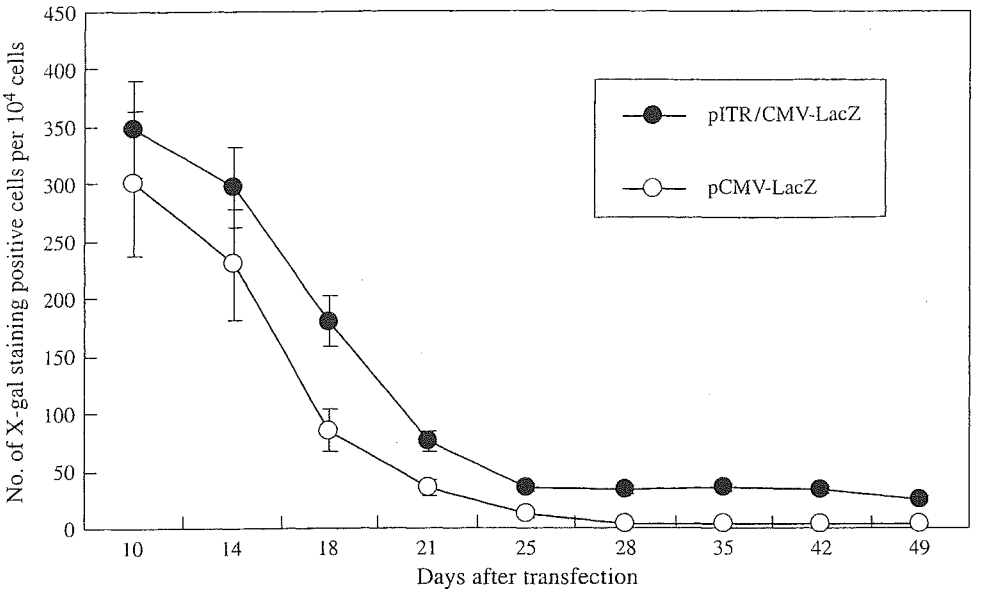

Figure 4. Long-term transfection study. HEK 293 cells were transfected with 2 μg of pITR/CMV-LacZ and pCMV-LacZ. At indicated time points, the cells were stained with X-gal and LacZ-positive cells were counted. Data are the average of two separate experiments

pITR-HIV or the mock plasmid. Furthermore, using anti-HIV Env mAb and anti-HIV Rev mAb alone did not bind to HIV Rev and HIV Env proteins, respectively. When 0.5 or 5 μg of each HIV Env-expressing plasmid was transfected into HEK 293 cells, similar HIV Env expression ratio of pITR/CMV-HIV to pCMV-HIV to using 2 μg DNA was observed (data not shown). These findings confirm the results shown in Figure 2, indicating that the ITR enhances CMV promoter function, which is independent of the transfected DNA plasmid dose.

The AAV ITRs are *cis*-acting elements that promote AAV integration to the host genome. To investigate whether the higher β-galactosidase activity of the pITR/CMV-LacZ was the result of chromosomal integration and/or episomal persistence, we transfected the pITR/CMV-LacZ or pCMV-LacZ plasmid to HEK 293 cells; cells were stained with X-gal at each passage and positive cells were counted. As shown in Figure 4, positive cells were greatly decreased from 10 days after transfection (usually we obtained 70% positive cells 2 days after transfection). Slightly higher numbers of positive cells were obtained in the pITR/CMV-LacZ-transfected cells than the pCMV-LacZ-transfected cells. By 49 days after transfection, there were 25 and 3 positive cells out of 10^4 cells in pITR/CMV-LacZ- and pCMV-LacZ-transfected cells, respectively. These data indicate that AAV ITRs may increase the chromosomal integration or episomal persistence.

Induction of HIV-specific immune responses *in vivo*

BALB/c mice were immunized and boosted twice with each HIV plasmid DNA construct. Analysis of the resultant serum Ab response showed that the antigen-specific IgG response peaked 10 weeks after the first immunization (Figure 5). The pITR/CMV-HIV plasmid induced significantly higher HIV-1-specific antibody than did any of the other plasmids examined.

ELIspot and tetramer assays were used to examine the effect of vaccination on Env-specific T cell activation. Mice immunized with pITR/CMV-HIV generated significantly more IFN-γ ELIspots (which reflect antigen-specific CTL activity) than animals immunized with pCMV-HIV (610 vs. 280 spots/10^6 cells, $p < 0.05$, Figure 6). Both of these treatments generated significantly more HIV-specific IFN-γ-secreting splenocytes than were present in the non-immune group (23 spots/10^6 cells) or pCMV-lacZ-immunized group (25 spots/10^6 cells). By use of a tetramer-binding assay (Figure 7), pITR/CMV-HIV plasmid induced two-fold more HIV Env-specific T cells than pITR/CMV-HIV (0.41% vs. 0.22%, $p < 0.05$).

Challenge experiments with vaccinia virus

To investigate whether the DNA vaccines can induce protective immunity against viral infection, the immune mice were intravenously challenged with recombinant vaccinia virus expressing the HIV *env* gene. DNA vaccines significantly reduced the viral loading (Figure 8); furthermore, the mice immunized with pITR/CMV-HIV plasmid showed more than five-fold lower viral loading than the mice with pCMV-HIV plasmid.

Discussion

Current results indicate that introduction of an AAV ITR into the regulatory region of plasmid DNA vaccines enhances CMV promoter activity, increases expression

Copyright © 2002 John Wiley & Sons, Ltd.

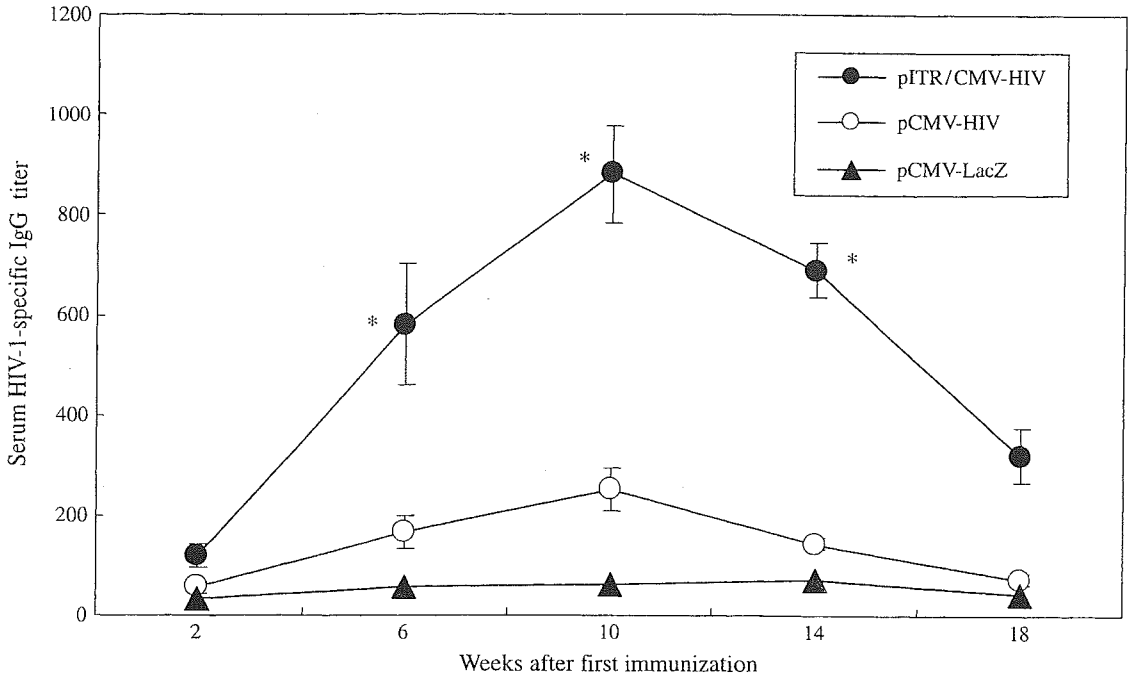

Figure 5. Anti-HIV serum IgG titers. Mice were immunized at 0, 2, and 4 weeks, and HIV-specific serum IgG titers monitored through week 18. Data represent the average of 5 mice/group. *Mean values significantly different from animals treated with pITR/CMV-HIV and pCMV-HIV plasmids

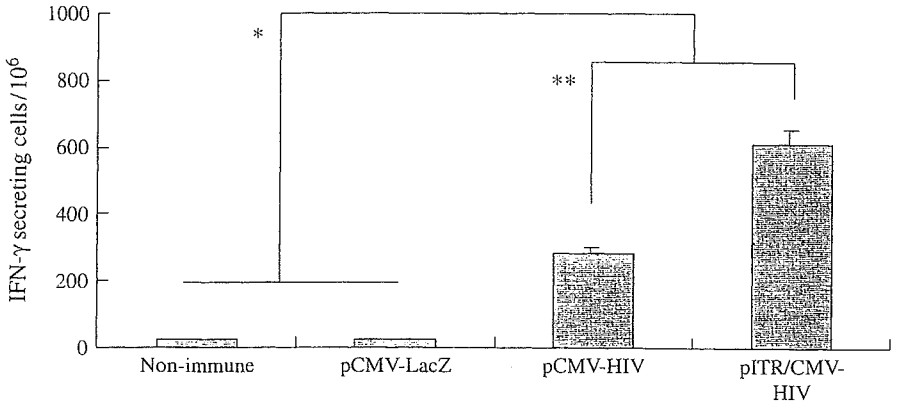

Figure 6. IFN-γ response of immunized mice. Mice were immunized as described in Figure 5. One week after the last immunization, spleen cells were isolated and stimulated *in vitro* with V3 peptide. The number of antigen-specific IFN-γ-secreting lymphocytes was determined by ELIspot assay. Data represent the average of 4 mice/group. *Mean values significantly different from animals treated with HIV Env-expressing plasmid and controls. **Mean values significantly different from animals treated with pITR/CMV-HIV and pCMV-HIV plasmids

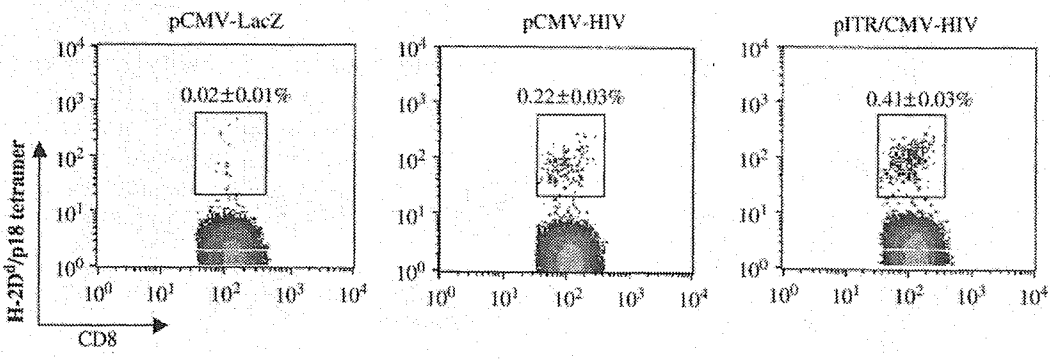

Figure 7. Frequency of HIV-specific CD8$^+$ spleen cells. Spleen cells from mice treated as described in Figure 6 were stained for CD8 expression, and for expression of TCR that recognized the MHC class I-restricted p18 tetramer from HIVgp160. Data represent the average of six mice

Copyright © 2002 John Wiley & Sons, Ltd.